

DESIGN OF AN ADAPTIVE BACKSTEPPING CONTROLLER FOR ACTIVE  
SUSPENSION SYSTEMS

by

Gökhan Kararsız

B.S., Mechanical Engineering, Yıldız Technical University, 2013

Submitted to the Institute for Graduate Studies in  
Science and Engineering in partial fulfillment of  
the requirements for the degree of  
Master of Science

Graduate Program in Mechanical Engineering  
Boğaziçi University

2017

## ACKNOWLEDGEMENTS

To begin with, I would like to express my gratitude to Assist. Prof. Halil İbrahim BAŞTÜRK for giving me the opportunity of this thesis. I am thankful for his great moral support and excellent academical guidance over past three years.

Secondly, thanks to everyone in Dynamics and Control Division at Yıldız Technical University. Especially, I would like to thank Prof. Rahmi GÜÇLÜ for believing and supporting my academic career, and I would also like to thank Assoc. Prof. Semih SEZER and Assist. Prof. Hakan YAZICI for their help throughout my undergraduate and graduate education. Special thanks go to Res. Assist. A. Oğuzhan AHAN for his criticism.

Finally, I would like to thank my parents who always have been there for me, unconditionally.

## ABSTRACT

### DESIGN OF AN ADAPTIVE BACKSTEPPING CONTROLLER FOR ACTIVE SUSPENSION SYSTEMS

This thesis presents a method to design an adaptive controller for active suspension systems which cancel the effect of the unknown road disturbance in presence of parametric uncertainty.

In this thesis, three different cases is investigated which are a seat, a quarter and a half vehicle models. The full state feedback is chosen for the seat and the quarter vehicle model since all states are available for measurement. In the half vehicle model, partial states are available for feedback. Therefore, state derivative feedback is employed. In addition, the dynamics of the actuator model is considered in the quarter and half car models. It is assumed that the applied force on the system depends on the current of the actuator. Since, the aim of the controller is to isolate the body from road disturbance, an adaptive controller is designed to regulate the current of the actuator.

The controller design is based on the following steps; the parametrization of the sinusoidal disturbance where the amplitude, the phase and the frequency is considered as unknown. Then an adaptive controller is designed to cancel the effect of the disturbance where the mass of the body and the parameters of suspension is considered as unknown. The backstepping procedure is employed due to the unmatched situation between the road disturbance and the actuator input. The stability of the controller is guaranteed with using the proposed lyapunov function. A simulation is shown to reveal the performance of the designed controller.

## ÖZET

# AKTİF SÜSPANSİYON SİSTEMLERİ İÇİN GERİ ADIMLAMA YÖNTEMİ KULLANILARAK UYARLAMALI KONTROLCÜ TASARIMI

Bu çalışmada aktif süspansiyon sistemleri için uyarlamalı kontrolcü tasarımı yapılmıştır. Kontrolcü tasarımı yapılırken, bozucu girişi belirsiz olarak kabul edilmiş ve taşıt gövdesinde yol bozukluğunun etkisini yok edecek şekilde tasarlanmıştır. Ayrıca, taşıt gövde kütlelerinin ve süspansiyon parametrelerinin belirsiz olduğu kabul edilmiştir.

Kontrolcünün performansını görmek için koltuk, çeyrek ve taşıt modellerinin dinamik modelleri elde edilmiş ve kontrolcü tasarımı yapılmıştır. İlerleyen bölümler aşağıdaki adımların takip edilmesi ile oluşturulmuştur; sinusoidal bozucunun parametrize edilmesi (burada genlik, faz ve frekansın bilinmediği kabulü yapılmıştır). Bozucunun, taşıt gövdesine iletilmeden yolcuların konforlu bir şekilde sağlanması için uyarlamalı kontrolcü tasarımı yapılmış ve asimptotik kararlılık önerilen Lyapunov fonksiyonu ile kanıtlanmıştır. Görsel örnek olması ve tasarlanan kontrolcünün performansını görebilmek için benzetim hazırlanmıştır.

## TABLE OF CONTENTS

ACKNOWLEDGEMENTS . . . . .	iii
ABSTRACT . . . . .	iv
ÖZET . . . . .	v
LIST OF FIGURES . . . . .	viii
LIST OF TABLES . . . . .	x
LIST OF SYMBOLS . . . . .	xi
LIST OF ACRONYMS/ABBREVIATIONS . . . . .	xiii
1. INTRODUCTION . . . . .	1
1.1. Background . . . . .	1
1.2. Literature Survey . . . . .	3
1.3. Problem Statement . . . . .	5
2. MATHEMATICAL MODELLING . . . . .	7
2.1. Quarter Car Model . . . . .	7
2.2. Half Car Model . . . . .	10
2.3. Actuator Model . . . . .	14
2.4. Disturbance Representation . . . . .	16
2.5. Random Road Input . . . . .	17
3. DESIGN OF AN ADAPTIVE BACKSTEPPING CONTROLLER FOR A SEAT MODEL WITH CONSIDERING KNOWN PARAMETERS . . . . .	19
3.1. Problem Statement . . . . .	19
3.2. Disturbance Representation . . . . .	21
3.3. Controller Design . . . . .	22
3.3.1. Isolating the seat from the road disturbance (Case 1) . . . . .	23
3.3.2. Suppressing the road disturbance (Case 2) . . . . .	23
3.4. Stability . . . . .	24
3.4.1. Case 1 . . . . .	24
3.4.2. Case 2 . . . . .	26
3.5. Simulation . . . . .	28

4. DESIGN OF AN ADAPTIVE BACKSTEPPING CONTROLLER FOR A QUARTER CAR MODEL WITH CONSIDERING PARAMETRIC UNCERTAINTY	32
4.1. Problem Statement	32
4.1.1. Model Assumptions	33
4.2. Disturbance Observer	34
4.3. Controller Design	36
4.4. Stability	38
4.5. Simulation	41
5. DESIGN OF AN ADAPTIVE BACKSTEPPING CONTROLLER FOR A HALF CAR MODEL WITH CONSIDERING PARAMETRIC UNCERTAINTY	45
5.1. Problem Statement	45
5.1.1. Model Assumptions	46
5.2. Road Disturbance Representation	47
5.3. Controller Design	49
5.4. Stability	55
5.5. Simulation	59
6. CASE STUDY	62
6.1. The Evaluation of RMS Value	63
7. CONCLUSIONS	68
REFERENCES	70
APPENDIX A: PARAMETERS OF THE SEAT MODEL	74
APPENDIX B: PARAMETERS OF THE QUARTER CAR MODEL	75
APPENDIX C: PARAMETERS OF THE HALF CAR	76
APPENDIX D: PARAMETERS OF THE ACTUATOR MODEL	77

## LIST OF FIGURES

Figure 1.1.	Ride comfort vs. vehicle handling for passive suspension conflict [7].	3
Figure 2.1.	Schematic sketch of a quarter car model. . . . .	8
Figure 2.2.	Schematic sketch of a half car model. . . . .	10
Figure 2.3.	Nonlinear spring behaviour [18]. . . . .	11
Figure 2.4.	Schematic sketch of the actuator model. . . . .	15
Figure 2.5.	The random disturbance input. . . . .	18
Figure 3.1.	Schematic illustration of a seat model. . . . .	20
Figure 3.2.	The acceleration response of the seat for case 1. . . . .	29
Figure 3.3.	The displacement response of the seat for case 1. . . . .	30
Figure 3.4.	The acceleration response of the seat for case 2. . . . .	30
Figure 3.5.	The displacement response of the seat for case 2. . . . .	31
Figure 3.6.	Applied control forces for case 1 and 2. . . . .	31
Figure 3.7.	Applied control forces for case 1 and 2. . . . .	31
Figure 4.1.	The displacement response of the body. . . . .	42

Figure 4.2.	The acceleration response of the body. . . . .	43
Figure 4.3.	Comparison between the adaptive controller and LQR for the displacement response of the body. . . . .	43
Figure 4.4.	Comparison between the adaptive controller and LQR for the acceleration response of the body. . . . .	44
Figure 5.1.	The displacement response of the body. . . . .	60
Figure 5.2.	The acceleration response of the body. . . . .	61
Figure 6.1.	The acceleration response of the body to random road input. . . . .	63
Figure 6.2.	Actuator responses. . . . .	64
Figure 6.3.	The displacement response of the body to random road input. . . . .	65
Figure 6.4.	Relative displacement between the body and the front tire. . . . .	65
Figure 6.5.	Relative displacement between the body and the rear tire. . . . .	66
Figure 6.6.	The angular acceleration of the pitch motion. . . . .	66
Figure 6.7.	The angular displacement of the pitch motion to random road input. . . . .	67
Figure 6.8.	The RMS values of heave acceleration for random road input. . . . .	67

## LIST OF TABLES

Table 2.1.	Parameters of the plant . . . . .	14
Table 6.1.	Road Roughness Values According to ISO 8608. . . . .	63
Table 6.2.	Comfort Reactions According to ISO 2631. . . . .	64
Table A.1.	Parameter values for the seat model. . . . .	74
Table B.1.	Parameter values for the quarter car model [28]. . . . .	75
Table C.1.	Parameter values for the half car model. . . . .	76
Table D.1.	Parameter values for the actuator [28]. . . . .	77

## LIST OF SYMBOLS

$A_i$	Amplitude
$a$	Lateral distance between the center of gravity and front tire for the half car model
$b$	Lateral distance between the center of gravity and rear tire for the half car model
$c_i$	Damping coefficient of the suspension
$e_i$	Error functions for backstepping method
$F_i$	Actuator Force
$G$	Chosen Hurwitz Matrix
$I_i$	Current of the actuator
$I_b$	Inertia of the body for the half car model
$K_i$	Force coefficient of the actuator
$K_e$	Velocity coefficient of the actuator
$k_i$	Stiffness coefficient of the suspension
$L_c$	Inductance coefficient of the actuator
$m$	Mass of the body for the seat model
$m_b$	Mass of the body for the half car model
$m_s$	Mass of the body for the quarter car model
$m_t$	Mass of the tire for quarter car model
$m_t^f$	Mass of the front tire for half car model
$m_t^r$	Mass of the rear tire for half car model
$n$	Number of distinct frequency
$R$	Resistance of the actuator
$T_l$	Kinetic Energy
$q_i$	Number of generalized coordinates
$Q_l$	Dissipative Energy
$V_l$	Potential Energy
$V_i$	Voltage of the actuator
$x$	Displacement of the body for the quarter car model

$\dot{x}$	Velocity of the body for the quarter car model
$\ddot{x}$	Acceleration of the body for the quarter car model
$x_t$	Displacement of the tire for the quarter car model
$\dot{x}_t$	Velocity of the tire for the quarter car model
$\ddot{x}_t$	Acceleration of the tire for the quarter car model
$x_b$	Displacement of the body for the half car model
$\dot{x}_b$	Velocity of the body for the half car model
$\ddot{x}_b$	Acceleration of the body for the half car model
$x_t^f$	Displacement of the front tire for the half car model
$\dot{x}_t^f$	Velocity of the front tire for the half car model
$\ddot{x}_t^f$	Acceleration of the front tire for the half car model
$x_t^r$	Displacement of the rear tire for the half car model
$\dot{x}_t^r$	Velocity of the rear tire for the half car model
$\ddot{x}_t^r$	Acceleration of the rear tire for the half car model
$x_t^r$	Displacement of the rear tire for the half car model
$\dot{x}_t^r$	Velocity of the rear tire for the half car model
$\ddot{x}_t^r$	Acceleration of the rear tire for the half car model
$x_{su}^r$	Displacement of the suspension gap tire for the half car model
$\dot{x}_{su}^r$	Velocity of the rear suspension gap for the half car model
$x_{su}^r$	Displacement of the rear suspension gap for the half car model
$\dot{x}_{su}^r$	Velocity of the rear suspension gap for the half car model
$\delta_i$	Error function for the observer
$\eta_i$	Observer filters for unknown parameters
$\varrho$	Pitch motion of the body for the half car model
$\dot{\varrho}$	Velocity of the pitch motion for the half car model
$\ddot{\varrho}$	Acceleration of the pitch motion for the half car model
$\xi_i$	Observer filters for known parameters
$\phi_i$	Phase
$\omega_i$	Frequency

**LIST OF ACRONYMS/ABBREVIATIONS**

<i>ISO</i>	International Organization for Standardization
<i>LQR</i>	Linear Quadratic Regulator
<i>RMS</i>	Root Mean Square
<i>PSD</i>	Power Spectral Density

# 1. INTRODUCTION

In today's market, there is a fierce competition among vehicle manufacturers. In order to attract customers' attention, manufacturers take advantage of mechatronic systems which enable to enhance road holding, performance and safety, such as, electronic stability control, anti-lock braking system, traction and suspension control systems [1]. In scope of this thesis, active suspension system is analysed.

Suspension system is one of the most important component in terms of vehicle dynamics [2]. It is the only part that contacts the road surface. Hence, the design of the suspension is crucial with respect to ride comfort and performance. In order to improve ride comfort, the main aim is to isolate the vehicle body from road irregularities [3]. To achieve that, the road induced vibration is not transmitted to the body. Researchers propose a method which the road disturbance is cancelled by applying a counter force with the help of an actuator.

Each year, more than 1.25 million people have been dead because of traffic accidents [4]. Therefore, a good suspension system should not only consider comfort but also provide safety. If the contact between tire and road is lost, driver cannot steer the vehicle. This situation is the cause of many accidents.

## 1.1. Background

Suspension systems are a vital part of vehicle dynamics. Early examples are used in horse-carriage systems. With the development of vehicles, the design of the suspension become more important due to high speeds. In literature, three different suspension system are proposed [5]. These are passive suspension, semi-active suspension and active suspension.

Passive suspension systems are consist of a spring and a damper. The duty of the spring is to provide a resisting force. The damper is used for dissipating the stored energy in the spring.

Manufacturers should provide excellent ride comfort as well as performance. However, there is a trade-off between ride comfort and performance in passive suspension system [6]. Perceived comfort by passengers can be altered by the parameters of the suspension. If the parameters of the suspension are set softly, in other words low damping, the passenger in the vehicle cabin is experience a comfortable ride. On the other hand, the cornering performance of vehicle is decrease due to soft suspension. In this configuration, when driver wants to turn a corner in high speed, one exhibits much more effort to keep the vehicle in the lane. Contrary, if the parameters of the suspension is set stiff or produced high damping, there is a bit increase cornering performance, but, road irregularities can be transmitted to vehicle body. Perceived comfort by passengers is decreased.

In passive suspension system, there is a conflict between performance and comfort, because of the inherent characteristic of the system. Thus, designers should consider this trade-off according to customer expectations and market position. In Figure 1.1, this conflict is shown [7].

To overcome this conflict, semi-active and active suspension systems are proposed. In order to provide comfort and performance simultaneously, semi-active suspension systems consist of a spring and a variable damper which adapts itself with respect to road so that the energy which induced by road is dissipated in the range of frequency of interest [8].

To eliminate the road disturbance, active suspension systems contain an actuator, in addition to a spring and a damper. The road disturbance is cancelled by applying a counter force with respect to the effect of the road. The actuator in the active suspension system provides the counter force. Therefore, the actuator plays an important role for the effectiveness of the controller.

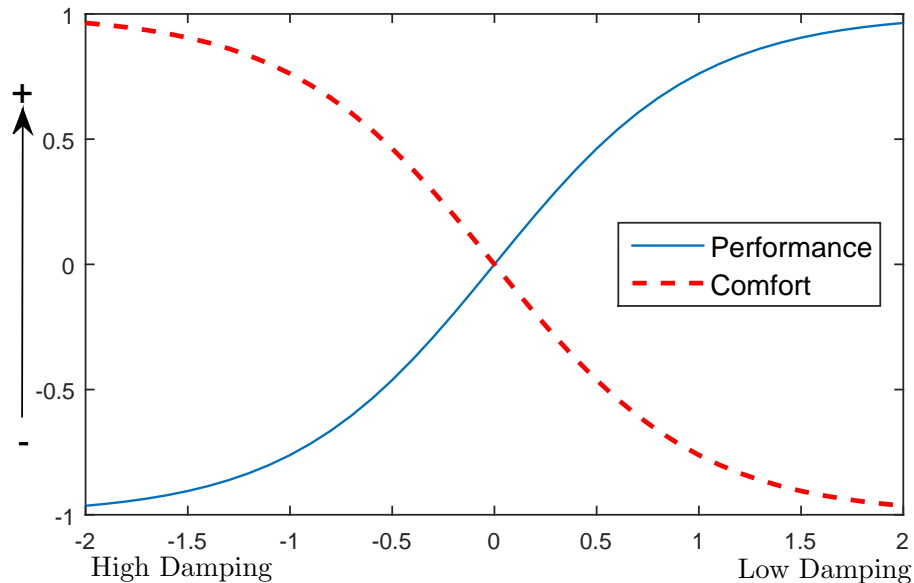


Figure 1.1. Ride comfort vs. vehicle handling for passive suspension conflict [7].

## 1.2. Literature Survey

The active suspension system has been investigated since 60's. Extensive studies are conducted to maintain comfort and safety such as;  $H_\infty$  [9], fuzzy logic [10] and sliding mode control [11]. However, the purpose of this thesis is the implementation of the adaptive backstepping approach. Thus, the survey is narrowed down with only adaptive backstepping method.

Additionally, there are ISO standards in the literature which related with the active suspension system. ISO 2631 focuses on the comfort of the passenger. It states that the vertical accelerations in between 0-2 hz. and 4-10 hz. affect the perceived comfort by the passengers [12]. ISO 8608 describes the generation of the random road profile. It is assumed that the road consists of a sum of sinusoidals.

In order to stabilize two subsystems, a backstepping method is developed by Petar V. Kokotovic [13]. The method is applied various applications, such as; robot control [14], quadcopter [15] and flight control systems [16]. This thesis presents the application of the backstepping method to active suspension systems.

In [17], Lin and Kanellakopoulos develop a nonlinear backstepping design with considering the nonlinear actuator dynamics. In [18], Lin and Huang apply the backstepping technique to a half-car model. They design two non-linear filters which limit suspension stroke. In [19], Yagiz and Hacıoglu use the full-car model to reveal the performance of the controller. In order to keep the vertical acceleration of the vehicle zero, they employ the reference tracking method. In simulation, numerical results is illustrated with time and frequency domain. The parametric uncertainty is not taking into account, but; a low pass filter is applied to the control signal. In [20], Karlson, Teel and Hrovat focus on the suspension stroke problem. They develop a a nonlinear adaptive controller considering the handling of the vehicle. The result is compared with LQ controller. In [21], Sun, Gao and Kaynak consider the parametric uncertainty. Because, the mass and inertia of the vehicle can be easily varied by the number of the passengers or payload. Therefore, they assume that the mass and the inertia is unknown, but, minimum and maximum values of mass and inertia are known. The spring nonlinearity and piecewise behaviour of the damper are taken into consideration. In [22], Sun, Pan, Zhang and Gao presents barrier Lyapunov function which allows to design a low conservatism nonlinear control technique with the enhanced ability to passenger comfort. In [23], Basturk uses the backstepping method to control the force of the actuator. In the design, the road disturbance is considered as unknown. The observer is designed to compensate the effect of the disturbance. To cancel the effect of the disturbance, a final sum of sinusoidal functions is modelled to represent the unknown road disturbance.

The given references above contribute to the literature, significantly. Among these papers, [19], [21], [22] and [23] are very fascinating and promising in terms of considering the parametric uncertainty, the road disturbance observer and the actuator dynamics. However, the combination of this three important problems is not taking into consideration, simultaneously. This situation motivates us that the literature needs a controller where the parametric uncertainties, the road disturbance observer and the actuator dynamics are considered at the same time.

### 1.3. Problem Statement

The aim of the active suspension is to isolate the vehicle body from road disturbances which induced by uneven terrain. To achieve that, a good active suspension system should provide improved ride comfort and improved road holding. The limitation, which is the lack of information about the road disturbance, is decreased the effectiveness of the control strategy. A new approach is developed for a control of the active suspension system under the unknown road disturbance where the parameters of the tire and mass are treated as known. Then, it is extended to unknown case.

One of our aim for the controller is unknown disturbance. Even though accelerometers are getting cheaper and more reliable [24], the cost of the system and noisy data are still problematic for automotive industry. Therefore, it is assumed that the road disturbance cannot be measured. To overcome the unknown disturbance, an observer is designed to compensate the road input. Furthermore, the road disturbance is assumed as a sinusoidal wave. According to ISO 2631, human body is sensitive to vibrations around 1 Hz and 10 Hz which enables that a final sum of sinusoidal functions is enough to represent the road disturbance. Therefore, we can use the model of disturbance in [25], where the model of the disturbance consists of a final sum of sinusoidal functions with unknown frequencies, amplitudes and phases [23].

Another challenge is uncertainties in the vehicle. The mass of the car body is considered as unknown because of the ambiguity of the vehicle load. The number of passenger and payload can be changed. In addition, due to the dynamic load (temperature fluctuation, tear and wear), the parameters of tire are uncertain. As a result, the coefficients of the tire are considered as unknown. Therefore, the unknown parameters are estimated by using update laws.

One of the most important part of the active suspension systems is the actuator which applies a force in order to compensate the effect of the disturbance. In this thesis, linear electromagnetic actuator will be used in the quarter and half car models. The electromagnetic force depends on the current of the actuator. Therefore, in order to combine two independent dynamics, backstepping approach will be used.

Although all needed parameters such as; accelerations, velocities and displacements of the body and tire can be available after filtering and integration operations in the test environment, the data lost is unavoidable after signal processing operation. The necessary information can be lost. This situation decreases the performance of the controller. It is assumed that partial states are available for measurement in the half car model to reduce the number of sensors.

It is a well-known fact that parameter uncertainty affects the performance of the controller drastically. Based on a Lyapunov theory, a new adaptive controller, which overcomes the uncertainties with adaptation law, will be designed. The asymptotic stability will be guaranteed.

In the light of above statements, this thesis is divided into three cases as follows. To begin with, a seat model, where the parametric uncertainty and the actuator dynamics are not taken into consideration, is studied. An adaptive controller for the seat model is designed by using full state feedback. Consequently, the road disturbance observer is designed for known parameters. Furthermore, a quarter car model is developed where the parameters of the tire and the body mass are treated as unknown and actuator dynamics is considered. Same as the seat model, the full state feedback is chosen for the controller. Lastly, a half car model is presented. Due to the complexity of the model, the both controllers are designed to control the heave and the pitch motion, where the dynamics of the actuator and unknown parameters for the body mass, the tire and also the actuator are considered. The road disturbance observer is designed for the both tire, separately.

## 2. MATHEMATICAL MODELLING

In this chapter, the mathematical models of the vehicle are discussed. In literature, quarter, half and full car models are developed to represent the motion of the body. Full car model is able to represent the heave, roll and pitch motion. However, the roll motion of the vehicle is neglected in the controller design. The effect of the roll motion is desired for the understeer behaviour. In scope of this thesis, half and quarter car models are investigated.

There are two different approaches to derive the equation of motion; Newtonian and Lagrangian approaches. In this thesis, Lagrangian approach is chosen for obtaining the equation of motion. Because of the fact that all models have a dissipative element, nonconservative Lagrangian Equation is considered. The derivation of the Lagrange equation is given in [26].

The expression of Lagrangian approach is given below,

$$\frac{d}{dt}\left(\frac{\partial L}{\partial \dot{q}}\right) - \left(\frac{\partial L}{\partial q}\right) = -\frac{\partial Q}{\partial \dot{q}} \quad (2.1)$$

where  $L = T - V$  which is the Lagrangian expression, T is the total kinetic energy and V is the total potential energy of the plant. Generalized coordinate of the plant is represented with q.

### 2.1. Quarter Car Model

Quarter car model represents the heave motion of the car. According to ISO 2631, humans are prone to more sensitive to vertical acceleration. Therefore, the quarter car model is sufficient to evaluate the comfort of the vehicle.

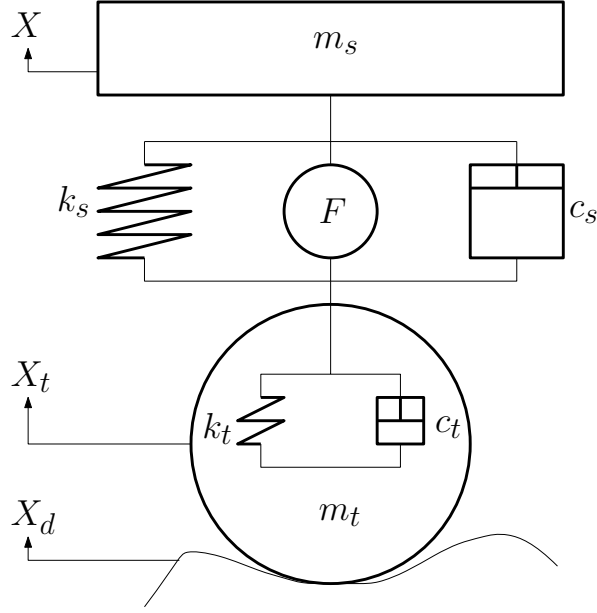


Figure 2.1. Schematic sketch of a quarter car model.

The schematic model is depicted in Figure 2.1, where  $m_s$  is the sprung mass, in other words, the mass of the body.  $m_t$  is the unsprung mass, in other words, the mass of the tire.  $k_s$  and  $k_t$  are the spring coefficients and  $c_s$  and  $c_t$  are the damping coefficients of the body and tire, respectively.  $F$  denotes the actuator input which placed in between body and tire and in parallel with the spring and the damper. The displacement and velocity is represented with  $x$  and  $\dot{x}$  for the body and  $x_t$  and  $\dot{x}_t$  for the tire, respectively.  $X_d$  denotes the road disturbance.

To derive the equations of motion for the quarter car, the plant is assumed to have two degrees of freedom. Therefore, the general coordinates of the plants are  $x$  and  $x_t$ .

Kinetic, potential energy and non conservative terms are given by;

$$T = \frac{1}{2}m\dot{x}^2 + \frac{1}{2}m_t\dot{x}_t^2 \quad (2.2)$$

$$V = \frac{1}{2}k(x - x_t)^2 + \frac{1}{2}k_t(x_t - x_d)^2 \quad (2.3)$$

$$Q = \left(\frac{1}{2}c(\dot{x} - \dot{x}_t)^2 + \frac{1}{2}c_t(\dot{x}_t - \dot{x}_d)^2\right) \quad (2.4)$$

Plugging (2.2) (2.3) and (2.4) into (2.1), the following is obtained for  $x$  and  $x_t$ , respectively.

$$\ddot{x} = -\frac{k}{m}(x - x_t) - \frac{c}{m}(\dot{x} - \dot{x}_t) + \frac{F}{m} \quad (2.5)$$

$$\ddot{x}_t = \frac{k}{m_t}(x - x_t) + \frac{c}{m_t}(\dot{x} - \dot{x}_t) - \frac{k_t}{m_t}(x_t - x_d) - \frac{c_t}{m_t}(\dot{x}_t - \dot{x}_d) - \frac{F}{m_t} \quad (2.6)$$

In state space form;

$$\dot{X} = A_0 X + B(\gamma^T(X - X_t) + \frac{F}{m_s}) \quad (2.7)$$

$$\dot{X}_t = A_0 X_t + B(\alpha^T X + \mu^T X_t + \kappa^T X_d - \frac{F}{m_t}) \quad (2.8)$$

where,

$$X = \begin{bmatrix} x & \dot{x} \end{bmatrix}^T \quad (2.9)$$

$$X_d = \begin{bmatrix} x_d & \dot{x}_d \end{bmatrix}^T \quad (2.10)$$

$$\gamma^T = \begin{bmatrix} -\frac{k}{m} & -\frac{c}{m} \end{bmatrix} \quad (2.11)$$

$$\alpha^T = \begin{bmatrix} \frac{k}{m_t} & \frac{c}{m_t} \end{bmatrix} \quad (2.12)$$

$$\mu^T = \begin{bmatrix} \frac{-k-k_t}{m_t} & \frac{-c-c_t}{m_t} \end{bmatrix} \quad (2.13)$$

$$\kappa^T = \begin{bmatrix} \frac{k_t}{m_t} & \frac{c_t}{m_t} \end{bmatrix} \quad (2.14)$$

$$A_0 = \begin{bmatrix} 0 & 1 \\ 0 & 0 \end{bmatrix} \quad (2.15)$$

$$B = \begin{bmatrix} 0 \\ 1 \end{bmatrix} \quad (2.16)$$

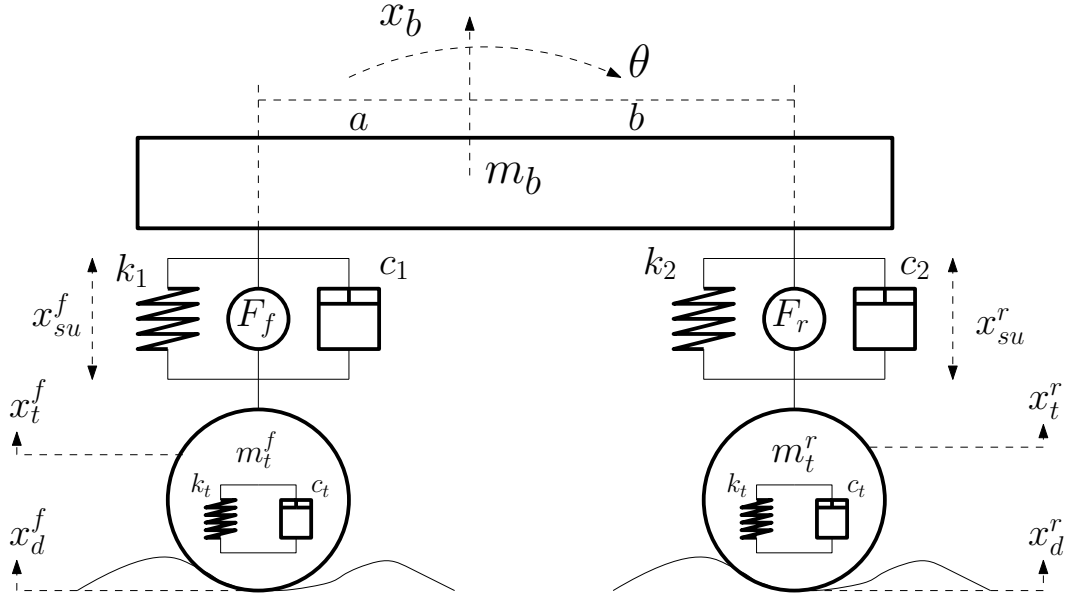


Figure 2.2. Schematic sketch of a half car model.

## 2.2. Half Car Model

The half car model consists of the body, the front and rear tires of vehicle which enable us to represent heave and pitch motion of vehicle. Figure 2.2 illustrates the half car model. There are two actuators which are placed in between the front and rear tires and the body. The combination of both actuator forces controls the pitch and the heave motions. The general coordinates are  $x_b$ ,  $x_t^f$ ,  $x_t^r$  and  $\varrho$ .

In this model, spring behaviour is considered as nonlinear. The method is taken from [27]. The force of the spring is obtained in the following. Firstly, nonlinear spring force can be represented as a power series.

$$F_{spring} = k_0 + k_1x + k_2x^2 + k_3x^3 + \dots \quad (2.17)$$

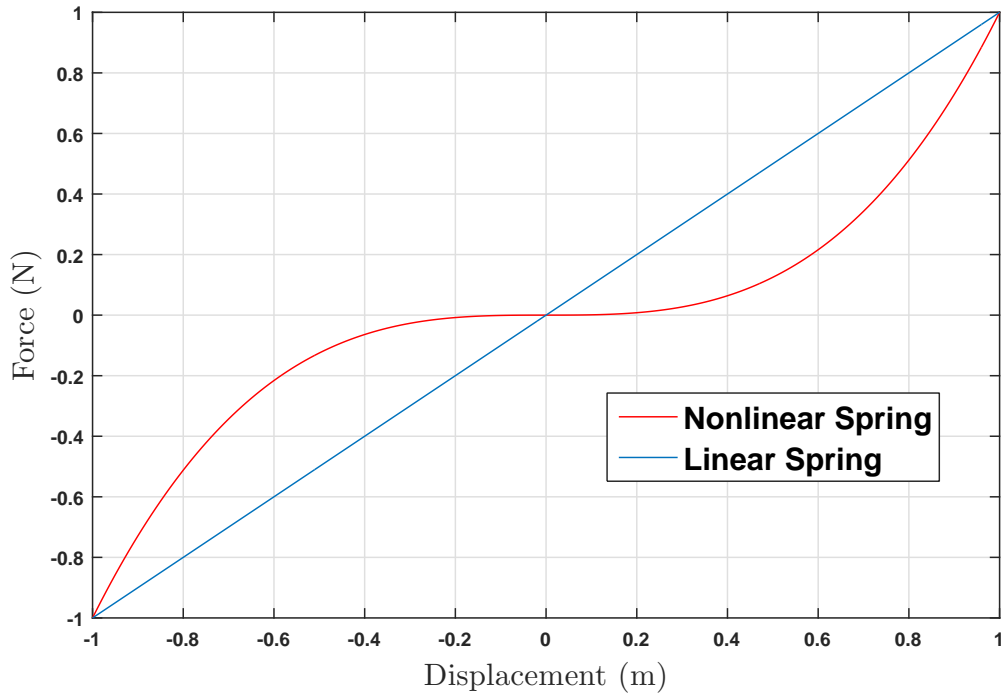


Figure 2.3. Nonlinear spring behaviour [18].

In (2.17),  $k_i$  (for  $i = 0, 1, 2, \dots$ ) is the nonlinear spring coefficient,  $x$  is the displacement of the nonlinear spring. To produce symmetric restoring force, an odd function ( $F(-x) = -F(x)$ ) is needed.

$$F_{spring} = k_1x + k_3x^3 + \dots \quad (2.18)$$

In Figure (2.3), nonlinear spring force versus the displacements is shown. To obtain the potential energy of the nonlinear spring, the area under the  $k$ - $x$  graph is integrated.

$$V_{spring} = \int_0^x F(u)du \quad (2.19)$$

where  $V$  is the potential energy,  $F$ , which depends on the dummy variable  $u$ , is the spring force.

Potential and kinetic energy and non conservative term of the plant is calculated as follows;

$$T = \frac{1}{2}m_b\dot{x}^2 + \frac{1}{2}I_b\dot{\theta}^2 + \frac{1}{2}m_t^f(\dot{x}_t^f)^2 + \frac{1}{2}m_t^r(\dot{x}_t^r)^2 \quad (2.20)$$

$$V = \frac{1}{2}k^f(x + a \sin \theta - x_t^f)^2 + \frac{1}{4}k_n^f(x + a \sin \theta - x_t^f)^4 + \frac{1}{2}k^r(x - b \sin \theta - x_t^r)^2 + \frac{1}{4}k_n^r(x - b \sin \theta - x_t^r)^2 + \frac{1}{2}k_t^f(x_t^f - x_d^f)^2 + \frac{1}{2}k_t^r(x_t^r - x_d^r)^2 \quad (2.21)$$

$$Q = \frac{1}{2}c^f(\dot{x} + a\dot{\theta} \cos \theta - \dot{x}_t^f)^2 + \frac{1}{2}c^r(\dot{x} - b\dot{\theta} \cos \theta - \dot{x}_t^r)^2 + \frac{1}{2}c_t^f(\dot{x}_t^f - \dot{x}_d^f)^2 + \frac{1}{2}c_t^r(\dot{x}_t^r - \dot{x}_d^r)^2 \quad (2.22)$$

Applying Lagrange equation to (2.20), (2.21) and (2.22),rearranging yields;

$$\begin{aligned} & m_b\ddot{x} + k^f(x + a \sin \varrho - x_t^f) + k_n^f(x + a \sin \varrho - x_t^f)^3 + k^r(x - b \sin \varrho - x_t^r) \\ & + k_n^r(x - b \sin \varrho - x_t^r)^3 + c^f(\dot{x} + a\dot{\varrho} \cos \varrho - \dot{x}_t^f) + c^r(\dot{x} - b\dot{\varrho} \cos \varrho - \dot{x}_t^r) \\ & = F_f + F_r \end{aligned} \quad (2.23)$$

$$\begin{aligned} & I_b\ddot{\theta} + k^f a \cos \varrho (x + a \sin \varrho - x_t^f) + k_n^f a \cos \varrho (x + a \sin \varrho - x_t^f)^3 \\ & - k^r b \cos \varrho (x - b \sin \varrho - x_t^r) - k_n^r b \cos \varrho (x - b \sin \varrho - x_t^r)^3 \\ & + c^f a \cos \varrho (\dot{x} + a\dot{\varrho} \cos \varrho - \dot{x}_t^f) - c^r b \cos \varrho (\dot{x} - b\dot{\varrho} \cos \varrho - \dot{x}_t^r) = -aF_f + bF_r \end{aligned} \quad (2.24)$$

$$\begin{aligned} & m_t^f \ddot{z}_t^f - k^f(x + a \sin \varrho - x_t^f) + k_t^f(x_t^f - x_d^f) - c^f(\dot{x} + a\dot{\varrho} \cos \varrho - \dot{x}_t^f) \\ & + c_t(\dot{x}_t^f - \dot{x}_d^f) = -F_f \end{aligned} \quad (2.25)$$

$$\begin{aligned} & m_t^r \ddot{x}_t^r - k^r(x - b \sin \varrho - x_t^r) + k_t^r(x_t^r - x_d^r) - c^r(\dot{x} - b\dot{\varrho} \cos \varrho - \dot{x}_t^r) \\ & + c_t(\dot{x}_t^r - \dot{x}_d^r) = -F_r \end{aligned} \quad (2.26)$$

Let the displacements and velocities for the suspensions are;

$$x_{su}^f = x + a \sin \varrho - x_t \quad (2.27)$$

$$x_{su}^r = x - b \sin \varrho - x_t^r \quad (2.28)$$

$$\dot{x}_{su}^f = \dot{x} + a\dot{\varrho} \cos \varrho - \dot{x}_t^f \quad (2.29)$$

$$\dot{x}_{su}^r = \dot{x} - b\dot{\varrho} \cos \varrho - \dot{x}_t^r \quad (2.30)$$

To ease the mathematical burden, small angle approximation is applied to pitch angle ( $\varrho$ ). We get,

$$x_{su}^f = x + a\varrho - x_t \quad (2.31)$$

$$x_{su}^r = x - b\varrho - x_t^r \quad (2.32)$$

$$\dot{x}_{su}^f = \dot{x} + a\dot{\varrho} - \dot{x}_t^f \quad (2.33)$$

$$\dot{x}_{su}^r = \dot{x} - b\dot{\varrho} - \dot{x}_t^r \quad (2.34)$$

where, assuming  $\cos \varrho \approx 1$  and  $\sin \varrho \approx \varrho$ . To represent the plant more compact form, the disturbance and the inputs are;

$$\nu_1 = -\frac{k_t^f}{m_t^f} x_d^f - \frac{c_t^f}{m_t^f} \dot{x}_d^f \quad (2.35)$$

$$\nu_2 = -\frac{k_t^r}{m_t^r} x_d^r - \frac{c_t^r}{m_t^r} \dot{x}_d^r \quad (2.36)$$

$$U_1 = F_f + F_r \quad (2.37)$$

$$U_2 = -aF_f + bF_r \quad (2.38)$$

Table 2.1. Parameters of the plant

$a_1 = -\frac{k^f}{m_b}$	$a_2 = -\frac{k^r}{m_b}$	$a_3 = -\frac{c^f}{m_b}$	$a_4 = -\frac{c^f}{m_b}$
$b_1 = -\frac{k^f a}{I_b}$	$b_2 = \frac{k^r b}{I_b}$	$b_3 = -\frac{c^f a}{I_b}$	$b_4 = \frac{c^b}{I_b}$
$c_1 = \frac{k^f}{m_t^f}$	$c_2 = -\frac{k_t^f}{m_t^f}$	$c_3 = \frac{c^f}{m_t^f}$	$c_4 = -\frac{c_t^f}{m_t^f}$
$d_1 = \frac{k^r}{m_t^r}$	$d_2 = -\frac{k_t^r}{m_t^r}$	$d_3 = \frac{c^r}{m_t^r}$	$d_4 = -\frac{c_t^r}{m_t^r}$
$a_{n1} = -\frac{k_n^f}{m_b}$	$a_{n2} = -\frac{k_n^r}{m}$	$b_{n1} = -\frac{k_n^f a}{I_b}$	$b_{n2} = \frac{k_n^r b}{I_b}$
	$c_{n1} = \frac{k_n^f}{m_t^f}$	$d_{n1} = \frac{k_n^r}{m_t^r}$	

Then, the plant can be rewritten as follows;

$$\begin{aligned}
\ddot{x}_b &= a_1(x_{su}^f)^3 + a_{n1}(x_{su}^f)^3 + a_2(x_{su}^r) + a_{n2}(x_{su}^r)^3 + a_3(\dot{x}_{su}^f) + a_4(\dot{x}_{su}^r) + \bar{m}_b U_1 \\
\ddot{q} &= b_1(x_{su}^f) + b_{n1}(x_{su}^f)^3 + b_2(x_{su}^r) + b_{n2}(x_{su}^r)^3 + b_3(\dot{x}_{su}^f) + b_4(\dot{x}_{su}^r) + \bar{I}_b U_2 \\
\ddot{x}_t^f &= c_1(x_{su}^f) + c_{n1}(x_{su}^f)^3 + c_2 \dot{x}_t^f + c_3(\dot{x}_{su}^f) + c_4 \dot{x}_t^f + \nu_1 - \frac{F_f}{m_t^f} \\
\ddot{x}_t^r &= d_1(x_{su}^r) + d_{n1}(x_{su}^r)^3 + d_2 \dot{x}_t^r + d_3(\dot{x}_{su}^r) + d_4 \dot{x}_t^r + \nu_2 - \frac{F_r}{m_t^r}
\end{aligned} \tag{2.39}$$

where  $\bar{m} = \frac{1}{m_b}$ ,  $\bar{I} = \frac{1}{I_b}$  is overparametrized. The rest of the parameters are given in Table 2.1.

### 2.3. Actuator Model

Actuator can be defined as the heart of the active suspension system. The duty of the actuator is to apply a counter force to overcome the effect of the road disturbances which gives an important role to actuator for the performance of the system. In the literature, actuators can be categorized as hydraulic, pneumatic and electromagnetic. Because of efficiency, easiness to control the applied force and dual operation of the actuator, electromagnetic actuator is chosen for our active suspension system. Detailed comparison of actuator types can be found in [28].

The actuator model is taken from [29] and [30]. The dynamics of the model is given by;

$$\dot{I}_i = \frac{1}{L_c} (V_i - I_i R - K_e \dot{x}_{su}^i) \quad (2.40)$$

The applied actuator force depends directly on the current, such that;

$$F_i = K_i I_i \quad (2.41)$$

where, subscript "i" denotes the number of the actuator.  $I$  is the current,  $K_i$  and  $K_e$  are the force and velocity coefficient, respectively.  $L_c$  and  $R$  represent the inductance and the resistance of the actuator, respectively.  $V$  is the voltage which is considered as the input of the plant in the controller design. Figure 2.4 depicts the schematic model of the actuator.

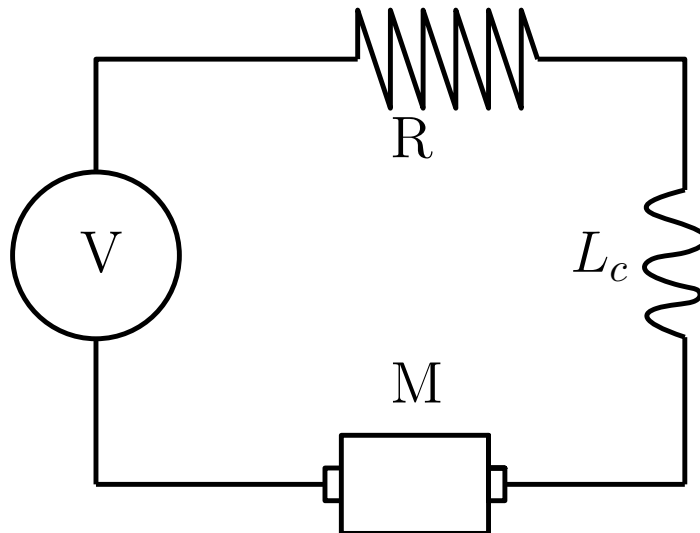


Figure 2.4. Schematic sketch of the actuator model.

## 2.4. Disturbance Representation

One of the objectives of this thesis is to cancel the effect of the disturbances despite unmeasured disturbance. We assume that the unknown disturbance consists of sum of sinusoidal where amplitude, frequency and phase is considered as unknown. Using the parametrization method which given in [24], [25] and [31] , we can design a disturbance observer for the plant (2.39) in the following.

The road disturbance is given by;

$$\nu = \sum_{i=1}^n A_i \sin(\omega_i t + \phi_i) \quad (2.42)$$

where amplitude ( $A_i$ ), frequency ( $\omega_i$ ) and phase ( $\phi_i$ ) is considered as unknown but the number of distinct frequency ( $n$ ) is known.

In our case, the number of distinct frequency is chosen 2. The first frequency represents the low frequency range in between 0.5-2 Hz., which cause motion sickness. Second frequency represents the high frequency range in between 4-10 Hz., which cause head toss.

The disturbance observer can be represented as the output of a linear exosystem;

$$\dot{P} = SP \quad \nu = h^T P \quad (2.43)$$

where  $P \in \mathbb{R}^{2q}$  is the state vector,  $S \in \mathbb{R}^{2q \times 2q}$  is the constant coefficient vector.  $l \in \mathbb{R}^{2q \times 2q}$  is chosen.

Consider the Sylvester equation,

$$MS - GM = lh^T. \quad (2.44)$$

If the spectrum of  $S$  and  $G$  are disjoint and  $(h^T, S)$  is observable with  $(G, l)$  controllable then the solution  $M$  is unique and invertible.

Multiplying (2.44) with  $P$ , by using state transformation  $w = MP$  and considering (2.27), we get;

$$M\dot{w} - Gw = l\nu. \quad (2.45)$$

Let  $G \in \mathbb{R}^{2q \times 2q}$  be a Hurwitz matrix and the  $(G, l)$  is controllable. Then the disturbance can be expressed as;

$$\dot{w} = Gw + l\nu \quad (2.46)$$

$$\nu = \theta^T w \quad (2.47)$$

where  $\theta^T = h^T M^{-1}$ .

## 2.5. Random Road Input

The road profile model is inspired from references [32] and [33]. It is assumed that the PSD (Power Spectral Densities) are employed to represent the road roughness.

The road profile is approximated in the following;

$$Sg(\Omega) = \begin{cases} \Omega \leq \Omega_0 & Sg(\Omega_0) \left( \frac{\Omega}{\Omega_0} \right)^{-n_1} \\ \Omega > \Omega_0 & Sg(\Omega_0) \left( \frac{\Omega}{\Omega_0} \right)^{-n_2} \end{cases} \quad (2.48)$$

where  $\Omega_0 = \frac{1}{2\pi}$  represents a reference frequency.  $\Omega$  denotes a frequency,  $n_1$  and  $n_2$  are the constants of the road.

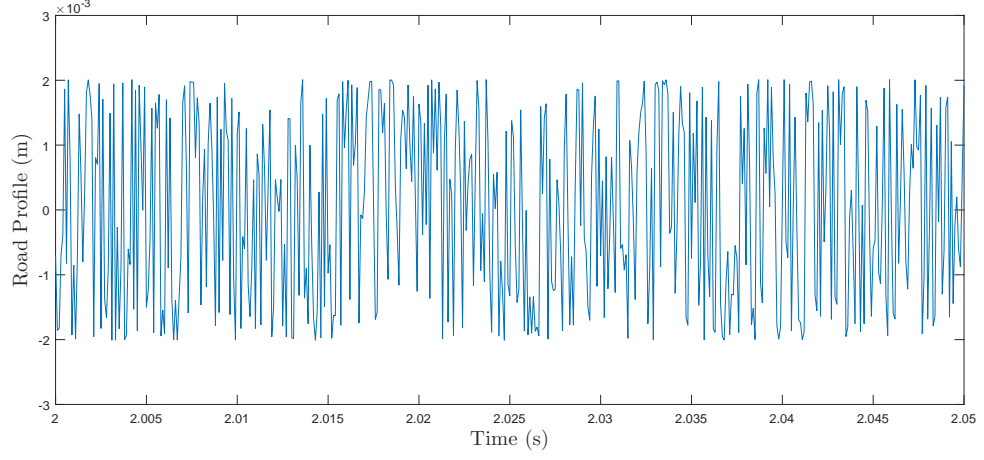


Figure 2.5. The random disturbance input.

Road roughness can be approximated by the following series;

$$X_d = \sum_{n=1}^{N_f} S_n \sin(nw_o t + \Phi_n) \quad (2.49)$$

where  $S_n = \sqrt{2S_g(n\Delta\Omega) \Delta\Omega}$ ,  $\Delta\Omega = \frac{2\pi}{L}$ .  $L$  is a distance of exposed road roughness,  $w_o = \frac{2\pi}{L}\nu_0$  and  $\Phi_n$  are considered as random variables within the interval  $[0, 2\pi)$ .  $N_f$  is a limit value of a considered frequency range. Figure 2.5 shows the random disturbance input.

### 3. DESIGN OF AN ADAPTIVE BACKSTEPPING CONTROLLER FOR A SEAT MODEL WITH CONSIDERING KNOWN PARAMETERS

In this chapter, an adaptive controller for a seat model is presented. The road disturbance is considered as unknown by the controller. Therefore, the observer is designed to compensate the effect of a sinusoidal disturbance. To estimate the road disturbance, the methodology, which is given in Section 2.4, is applied to the seat model by using full state measurement. The plant is parametrized as an output of an known feedback system. Then, the controller is designed. The stability of the controller is established by using proposed Lyapunov function.

The application of the active suspension control on the seat model is illustrated in Figure 3.1. This approach is more suitable to larger vehicles such as trucks, because, the performance of the vehicle is not demanded from customers in this segment. In addition, high energy consumption due to control large masses, decreases the change of applicability.

#### 3.1. Problem Statement

Let us consider the given model in Figure 3.1. The plant has a single degree of freedom which represents the seat of a vehicle. The controller aim is to regulate the seat of the vehicle.

The equation of motion of the plant is given by;

$$m\ddot{x} + k(x - x_d) + c(\dot{x} - \dot{x}_d) = F \quad (3.1)$$

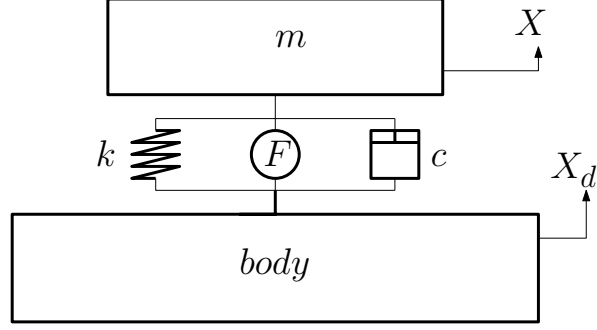


Figure 3.1. Schematic illustration of a seat model.

In (3.1),  $X$  and  $\dot{X}$  represent the vertical displacement and velocity of the seat, the actuator input is represented by  $F$ .  $k$  and  $c$  are the damping and spring coefficients, respectively.  $X_d$  and  $\dot{x}_d$  is the road inputs.

$$\dot{X} = A_0 X + B(\alpha^T X + \nu + \frac{F}{m}) \quad (3.2)$$

where;

$$A_0 = \begin{bmatrix} 0 & 1 \\ 0 & 0 \end{bmatrix} \quad (3.3)$$

$$B = \begin{bmatrix} 0 \\ 1 \end{bmatrix} \quad (3.4)$$

$$\alpha^T = \begin{bmatrix} \frac{k}{m} & \frac{c}{m} \end{bmatrix} \quad (3.5)$$

$$X = \begin{bmatrix} x \\ \dot{x} \end{bmatrix} \quad (3.6)$$

$$\nu = \begin{bmatrix} \frac{k}{m} & \frac{c}{m} \end{bmatrix} \begin{bmatrix} x_d \\ \dot{x}_d \end{bmatrix}. \quad (3.7)$$

**Model Assumptions:**

- All states are available for measurement except the disturbance.
- The parameters of the system are known.
- The actuator dynamics is not taking into account.  $F$  is assumed directly applied to the plant.

**3.2. Disturbance Representation**

In Section 2.4, the modelling procedure of the road disturbance is given. In this section, the procedure is applied to the plant (3.2).

**Lemma 3.1.** *The disturbance observer is proposed as;*

$$\nu = \theta^T \delta + \theta^T \xi. \quad (3.8)$$

*The filters are;*

$$\xi = \eta + NX \quad (3.9)$$

$$\dot{\eta} = G\xi - (NA_0X + l(-\frac{k}{m}x - \frac{c}{m}\dot{x} + \frac{F}{m})). \quad (3.10)$$

*Note that the following is obtained by plugging (3.10) and (3.2) into (3.9).*

$$\dot{\xi} = G\xi + l\nu \quad (3.11)$$

*Proof.* Define an estimation error;

$$\delta = w - \xi \quad (3.12)$$

where the dynamics of  $w$  is given in Section 2.4.

Considering the equation (2.47); taking the time derivative of  $\delta$ ,

$$\dot{\delta} = Gw + l\nu - (\dot{\eta} + N(A_0X + B(-\frac{k}{m}x - \frac{c}{m}\dot{x} + \nu + \frac{F}{m}))). \quad (3.13)$$

Substituting (3.10) into (3.13), we get

$$\dot{\delta} = G\delta. \quad (3.14)$$

Considering  $G$  is a Hurwitz matrix, we conclude that  $\delta \rightarrow 0$  when  $t \rightarrow \infty$ .  $\square$

The following plant dynamics is obtained by plugging (3.8) into (3.2).

$$\dot{X} = A_0X + B(\alpha^T X + \theta^T \delta + \theta^T \xi + \frac{F}{m}) \quad (3.15)$$

### 3.3. Controller Design

Since the force of the actuator affects both the body and the seat, the design of the controller is focused on either isolating the seat from the road disturbance or suppressing the road disturbance while neglecting the motion of the seat. In this section, both cases are investigated.

### 3.3.1. Isolating the seat from the road disturbance (Case 1)

The actuator force regulates the motion of the seat. To control the acceleration of the seat, the proposed adaptive controller is designed for the input term  $F$ , considering the plant dynamics (3.15) and the model assumptions. The desired  $F$  is;

$$F = m(KX - \alpha^T X - \hat{\theta}^T \xi) \quad (3.16)$$

where  $K \in \mathbb{R}^{1 \times q}$  is a controller gain matrix which is chosen. Using the certainty of equivalence,  $\hat{\theta}^T$  is the estimation of  $\theta^T$  which obeys,

$$\tilde{\theta}^T = \theta^T - \hat{\theta}^T. \quad (3.17)$$

The update law;

$$\dot{\hat{\theta}} = \gamma X^T P B \xi \quad (3.18)$$

where  $\gamma$  is the update gain and  $P$  is the solution of the matrix;

$$(A_0 + BK)^T P + P^T (A_0 + BK) = -2I \quad (3.19)$$

### 3.3.2. Suppressing the road disturbance (Case 2)

In this case, the controller is designed for suppressing the road disturbance. The following actuator input is proposed to cancel the effect of disturbance.

$$F = m(-\hat{\theta}^T \xi) \quad (3.20)$$

The update law;

$$\dot{\hat{\theta}} = \gamma X^T P B \xi \quad (3.21)$$

where  $\gamma$  is the update gain and  $P$  is the solution of the matrix;

$$(A_0 + B\alpha^T)^T P + P^T (A_0 + B\alpha^T) = -2I \quad (3.22)$$

### 3.4. Stability

The following theorems assure the stability of the proposed controllers.

#### 3.4.1. Case 1

**Theorem 3.2.** *Considering the plant (3.2) which consists of the adaptive controller (3.16), the update law (3.18) and the observer for the road disturbance (3.8). In view of the model assumptions,*

- (i) *The equilibrium  $X = \delta = 0$  is stable and the signals  $x$ ,  $\dot{x}$  and  $\delta$  converge to zero while time goes to  $\infty$ .*
- (ii) *The signal  $F$  is bounded for all initial conditions.*

*Proof.* Plugging (3.15) into the plant (3.2), the following closed-loop system is obtained;

$$\dot{X} = (A_0 + BK)X + B(\tilde{\theta}^T \xi + \theta^T \delta) \quad (3.23)$$

The following Lyapunov candidate is chosen to establish the stability of the closed-loop system (3.23);

$$V = \frac{1}{2} \left( X^T P X + \frac{1}{\gamma} \tilde{\theta}^T \tilde{\theta} + \delta^T P_G \delta \right) \quad (3.24)$$

where;

$$G^T P_G + P_G G = -2\varepsilon I \quad (3.25)$$

Taking the derivative of  $V$  with respect to time, taking into account of (3.14), (3.18) and (3.23) yields;

$$\dot{V} = -X^T X - \varepsilon \delta^T \delta + X^T P B \theta^T \delta \quad (3.26)$$

To get rid of the cross term, Young's inequality [13] is applied as follows;

$$X^T P B \theta^T \delta \leq \frac{X^T X}{2} + \frac{\delta^T \theta B^T P P B \theta^T \delta}{2} \quad (3.27)$$

$$X^T P B \theta^T \delta \leq \frac{X^T X}{2} + \lambda_{\max}(\theta B^T P P B \theta^T) \delta^T \delta \quad (3.28)$$

Plugging (3.28) into (3.26) and choosing  $b = \lambda_{\max}(\theta B^T P P B \theta^T)$  and  $\varepsilon = 1 + b$ , we get;

$$\dot{V} \leq -X^T X - \delta^T \delta \quad (3.29)$$

Then, it is concluded the following;

$$V(t) \leq V(0) \quad (3.30)$$

Defining;

$$\mathcal{U} = \begin{bmatrix} X & \delta & \tilde{\theta} \end{bmatrix}^T \quad (3.31)$$

Considering (3.30), the following function is obtained;

$$|\mathcal{U}|^2 \leq M_1 |\mathcal{U}(0)|^2 \quad (3.32)$$

where  $M_1 > 0$ ,

$\forall \mathcal{U}$ , (3.14), (3.18) and (3.23) are continuous in  $\mathcal{U}$  and  $t$ , which tells us that (3.29) is continuous in  $\mathcal{U}$  and  $t$ . Considering (3.30),  $\mathcal{U}$  is bounded. By using Lasalle-Yoshisawa theorem [13],  $\dot{V}$  ensures that  $X$  and  $\delta$  converge to zero while time goes to  $\infty$ . From the boundedness of  $\mathcal{U}$  and the convergence of  $X$  and  $\delta$ , it assures that  $\dot{X}$  is bounded.

By virtue of the assumption of the disturbance,  $\nu$  is bounded. Then, considering  $G$  is Hurwitz, we conclude that  $w$  is bounded with using (2.47). In view of (3.17),  $\xi$  is bounded. Moreover, Considering (3.17) and the boundedness of  $\tilde{\theta}$ ,  $\hat{\theta}$  is bounded. Finally, it also tells us that  $F$  is also bounded with considering (3.16).  $\square$

### 3.4.2. Case 2

**Theorem 3.3.** *Considering the plant (3.2) which consists of the adaptive controller (3.20), the update law (3.21) and the observer for the road disturbance (3.8). In view of the model assumptions,*

- (i) *The equilibrium  $X = \delta = 0$  is stable and the signal  $\delta$  converges to zero while time goes to  $\infty$ .*
- (ii) *The signal  $F$  is bounded for all initial conditions.*

*Proof.* Plugging (3.20) into the plant (3.15), the following closed-loop system is obtained;

$$\dot{X} = (A_0 + B\alpha^T)X + B(\tilde{\theta}^T\xi + \theta^T\delta) \quad (3.33)$$

The following Lyapunov candidate is chosen to establish the stability of the closed-loop system (3.33)

$$V = X^T P X + \frac{1}{\gamma} \tilde{\theta}^T \tilde{\theta} + \delta^T P_G \delta \quad (3.34)$$

where;

$$G^T P_G + P_G P = -2\varepsilon I \quad (3.35)$$

Taking the derivative of  $V$  with respect to time, taking into account of (3.14), (3.21) and (3.33) yields;

$$\dot{V} = -X^T X - \varepsilon \delta^T \delta + X^T P B \theta^T \delta \quad (3.36)$$

To get rid of the cross term, Young's inequality [13] is applied as follows;

$$X^T P B \theta^T \delta \leq \frac{X^T X}{2} + \frac{\delta^T \theta B^T P P B \theta^T \delta}{2} \quad (3.37)$$

$$X^T P B \theta^T \delta \leq \frac{X^T X}{2} + \lambda_{\max}(\theta B^T P P B \theta^T) \delta^T \delta \quad (3.38)$$

Plugging (3.38) into (3.36) and choosing  $b = \lambda_{\max}(\theta B^T P P B \theta^T)$  and  $\varepsilon = 1 + b$ , we get;

$$\dot{V} \leq -X^T X - \delta^T \delta \quad (3.39)$$

Then, it is concluded;

$$V(t) \leq V(0) \quad (3.40)$$

Defining;

$$\mathcal{U} = \begin{bmatrix} X & \delta & \tilde{\theta} \end{bmatrix}^T \quad (3.41)$$

Considering (3.40), the following is obtained;

$$|\mathcal{U}|^2 \leq M_1 |\mathcal{U}(0)|^2 \quad (3.42)$$

where  $M_1 > 0$ ,

$\forall \mathcal{U}$ , (3.14), (3.21) and (3.33) are continuous in  $\mathcal{U}$  and  $t$ , which tells us that (3.39) is continuous in  $\mathcal{U}$  and  $t$ . Considering (3.40),  $\mathcal{U}$  is bounded. By using Lasalle-Yoshisawa theorem [13],  $\dot{V}$  ensures that  $X$  and  $\delta$  converge to zero while time goes to  $\infty$ . From the boundedness of  $\mathcal{U}$  and the convergence of  $X$  and  $\delta$ , it assures that  $\dot{X}$  is bounded.

By virtue of the assumption of the disturbance,  $\nu$  is bounded. Then, considering  $G$  is Hurwitz, we conclude that  $w$  is bounded with using (2.47). In view of (3.17),  $\xi$  is bounded. Moreover, considering (3.17) and the boundedness of  $\tilde{\theta}$ ,  $\hat{\theta}$  is bounded. Finally, it also tells us that  $F$  is also bounded with considering (3.16).  $\square$

### 3.5. Simulation

In order to reveal the performance of the controller, the following road test simulation is applied. The model parameters are  $m = 320kg$ ,  $k = 18000\frac{N}{m}$ ,  $c = 1000\frac{N}{ms}$ . The controller and update gains are chosen as  $K = [-2000 \ -3000]$  and  $\gamma = 200$ , respectively. The observer parameters are  $l = [1 \ 2 \ 3 \ 4]^T$  and  $G = \begin{bmatrix} -1 & 0 & 0 & 0 \\ 0 & -2 & 0 & 0 \\ 0 & 0 & -3 & 0 \\ 0 & 0 & 0 & -4 \end{bmatrix}$ . Initial conditions are assumed as zeros.

The road disturbance is represented with the following function;

$$X_{d1} = 0.03 \sin(2\pi t + \frac{\pi}{6}) + 0.01 \sin(5\pi t) \quad (3.43)$$

where the road input (3.43) consists of two distinct frequencies.

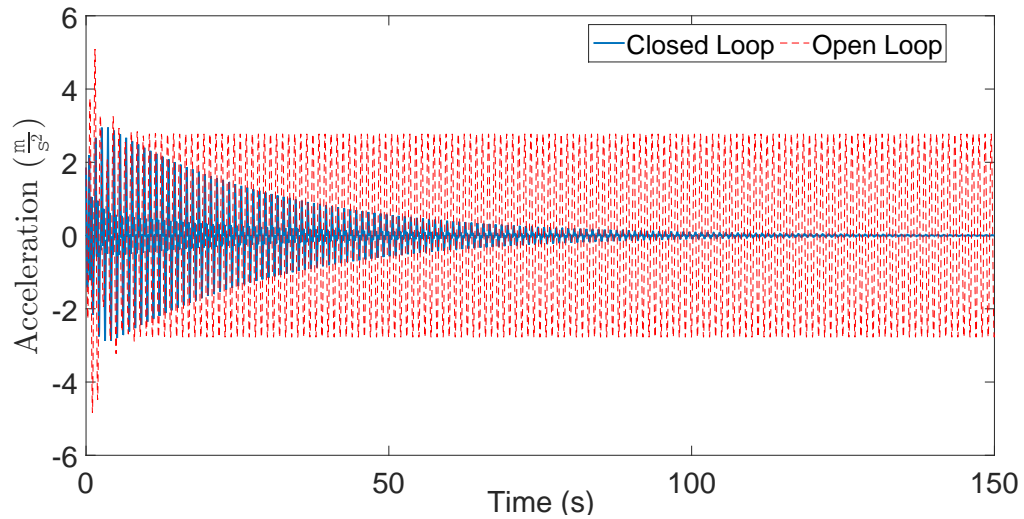


Figure 3.2. The acceleration response of the seat for case 1.

Figures 3.2 and 3.3, illustrate the vertical acceleration and the displacement of the seat with respect to time for case 1 and case 2, respectively. Red dashed lines represent open loop responses. Blue lines represent closed loop responses. It is clear that the closed loop responses of the seat are strictly decreased comparing the open loop responses for both cases. Additionally, the acceleration and the displacement responses for case 1 and case 2 converge to zero, perfectly. Desired comfort is achieved in the steady state response for both cases. Nevertheless, case 2 converge to zero more quickly than the case 1. Moreover, Figure 3.6 and 3.7 illustrates the force response for case 1 and case 1, respectively. Considering the Figure 3.7, case 2 needs much less actuator force which leads to lower energy consumption than case 1.

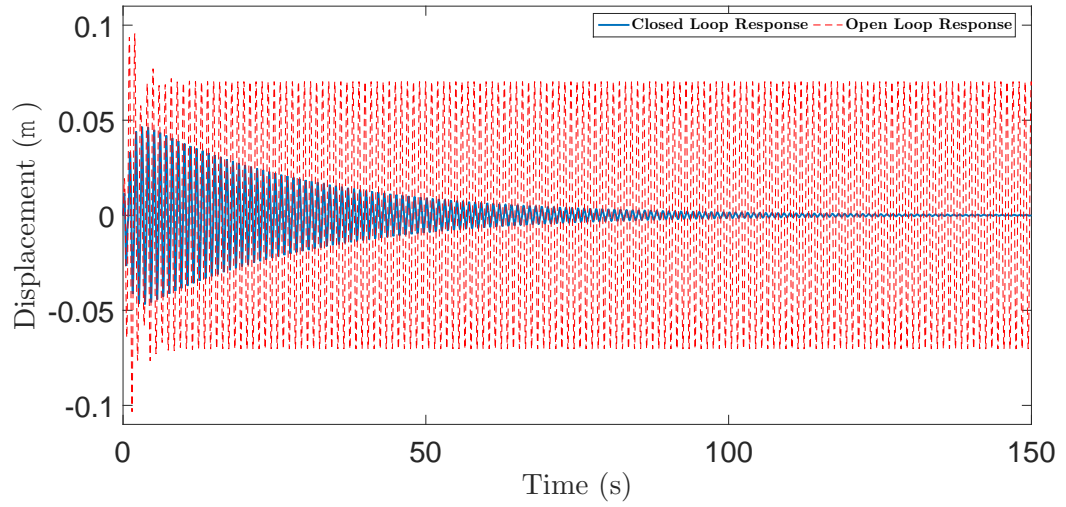


Figure 3.3. The displacement response of the seat for case 1.

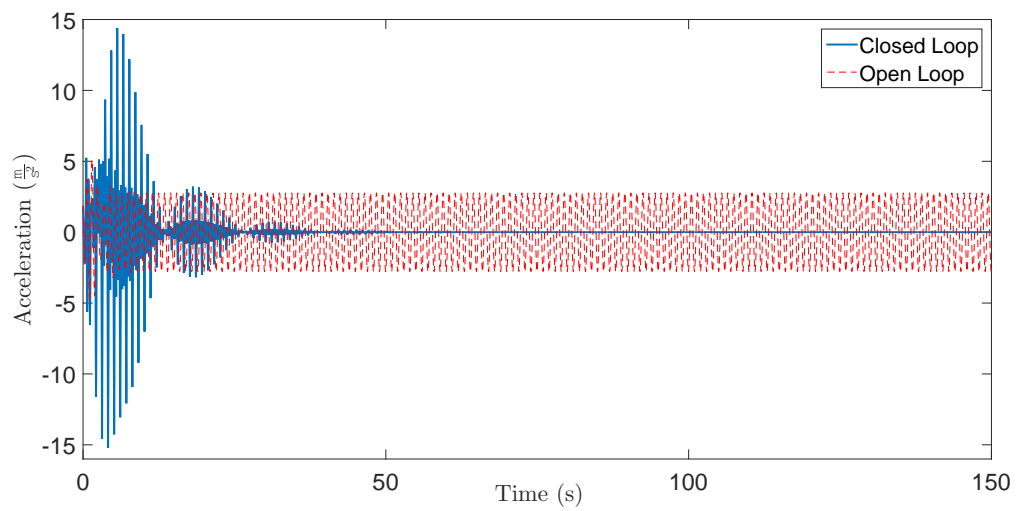


Figure 3.4. The acceleration response of the seat for case 2.

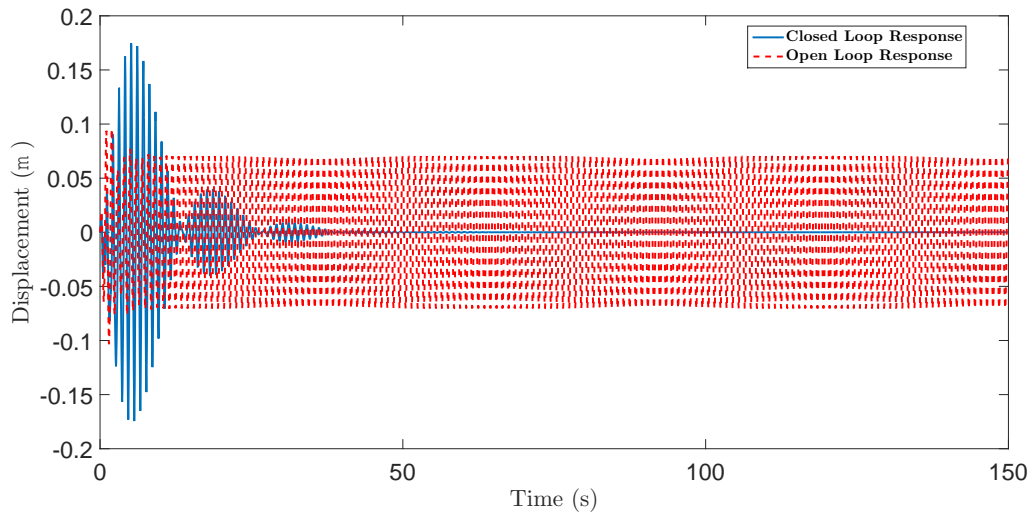


Figure 3.5. The displacement response of the seat for case 2.

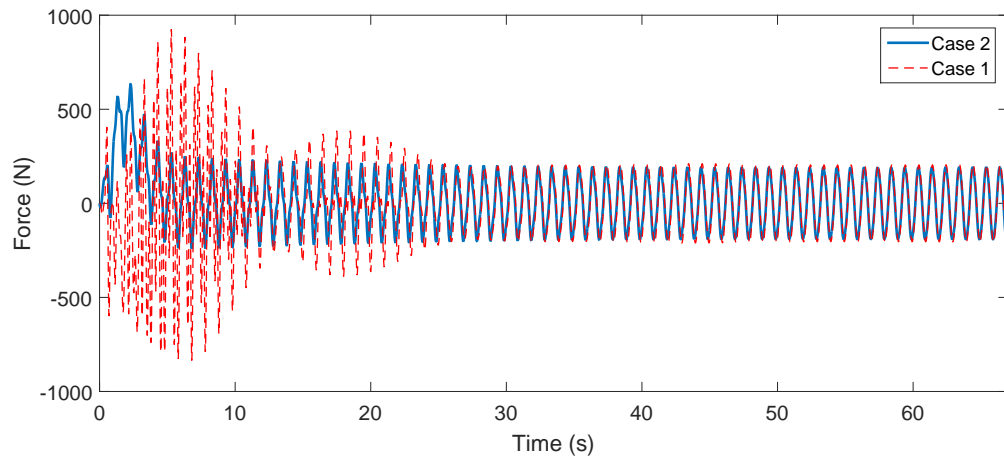


Figure 3.6. Applied control forces for case 1 and 2.

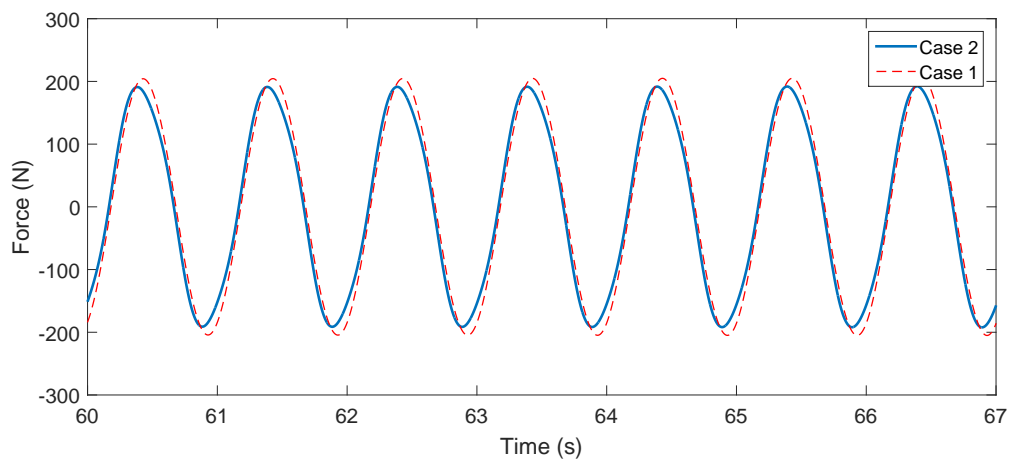


Figure 3.7. Applied control forces for case 1 and 2.

## 4. DESIGN OF AN ADAPTIVE BACKSTEPPING CONTROLLER FOR A QUARTER CAR MODEL WITH CONSIDERING PARAMETRIC UNCERTAINTY

In this section, an adaptive backstepping controller is applied to the quarter car model where the mass of the body, the damping and spring coefficients of tire is unknown. In addition, the road disturbance can not be measured. Therefore, the road disturbance observer is designed same as Section 3. Since the parameters of the vehicle are considered as unknown, the designed observer for the seat model cannot be used. In order to derive the new observer, new filters are introduced. Another improvement of this section is the actuator dynamics. In previous section, it is assumed that the force of the actuator is directly applied to the system. The dynamics of the actuator is neglected. Here, the electromagnetic actuator dynamics is included in the quarter car model.

### 4.1. Problem Statement

The aim of the proposed controller is to regulate the vertical body motion despite the effect of the disturbance. The motion of the tire is not taken into consideration. However, it is assumed that the vertical displacement of the tire is within the suspension stroke limit.

The derivation of the quarter car model is discussed in Section 2.1. The equation of motion for the body and the tire is obtained in (2.5). The electromagnetic actuator model is taken from (2.40).

#### 4.1.1. Model Assumptions

- It is assumed that damper and spring characteristics are taking into account as linear.
- All states are available for measurement except the disturbance.
- The mass of the body and the damping and spring coefficients of the tire is considered as unknown.
- The actuator dynamics is considered.
- The relative displacement between the body ( $X$ ) and the tire ( $X_t$ ) is limited within the suspension gap.

Let us recall that the dynamics of the quarter vehicle model which is derived in Section 2.1;

$$\begin{aligned}\dot{X} &= A_0 X + B(\gamma^T(X - X_t) + \frac{F}{m_s}) \\ \dot{X}_t &= A_0 X_t + B(\alpha^T X + \mu^T X_t + \nu - \frac{F}{m_t})\end{aligned}\quad (4.1)$$

where;

$$X = \begin{bmatrix} x_s & \dot{x}_s \end{bmatrix}^T \quad (4.2)$$

$$X_t = \begin{bmatrix} x_t & \dot{x}_t \end{bmatrix}^T \quad (4.3)$$

$$\gamma^T = \begin{bmatrix} -\frac{k}{m} & -\frac{c}{m} \end{bmatrix} \quad (4.4)$$

$$\alpha^T = \begin{bmatrix} \frac{k}{m_t} & \frac{c}{m_t} \end{bmatrix} \quad (4.5)$$

$$\mu^T = \begin{bmatrix} \frac{-k-k_t}{m_t} & \frac{-c-c_t}{m_t} \end{bmatrix} \quad (4.6)$$

$$\nu = \begin{bmatrix} \frac{k_t}{m_t} & \frac{c_t}{m_t} \end{bmatrix} \begin{bmatrix} x_d \\ \dot{x}_d \end{bmatrix} \quad (4.7)$$

$$A_0 = \begin{bmatrix} 0 & 1 \\ 0 & 0 \end{bmatrix} \quad (4.8)$$

$$B = \begin{bmatrix} 0 & 1 \end{bmatrix}^T. \quad (4.9)$$

The schematic model is depicted in Figure 2.1, where  $m$  is the sprung mass, in other words, the mass of the body.  $m_t$  is the unsprung mass, in other words, the mass of the tire.  $k_s$  and  $k_t$  are the spring coefficients and  $c_s$  and  $c_t$  are the damping coefficients of the body and tire, respectively.  $F$  denotes the actuator input which is placed in between body and tire and in parallel with the spring and the damper. The displacement and velocity is represented with  $x$  and  $\dot{x}$  for the body and  $x_t$  and  $\dot{x}_t$  for the tire, respectively.

## 4.2. Disturbance Observer

To represent the unknown disturbance, the parametrization process, which is given in Section 2.4, is applied to the quarter car model. Considering the model (2.5), the unknown parameters in the dynamics of the tire (4.16) makes impossible to apply the method in Section 3.2. In order to handle the unknown terms, the observer, which uses multiple filters, is designed.

**Lemma 4.1.** *The disturbance observer is given as follows;*

$$\nu = \theta^T \delta + \theta^T \xi + \beta_1^T \eta_1 + \beta_2^T \eta_2 \quad (4.10)$$

where the filters are;

$$\begin{aligned} \xi &= \eta + NX_t \\ \dot{\eta} &= G\xi - N\left(A_0X_t + B\left(\alpha^T X - \frac{F}{m_t}\right)\right) \\ \dot{\eta}_1 &= G\eta_1 - lX_t \\ \dot{\eta}_2 &= G\eta_2 - l\dot{X}_t \end{aligned} \quad (4.11)$$

The filters  $\eta_1$  and  $\eta_2$  are designed to overcome the unknown terms which are  $\frac{k_t}{m_t}$  and  $\frac{c_t}{m_t}$ .

*Proof.* Define an estimation error;

$$\delta = w - \left( \xi + \frac{-k_t - k_s}{m_t} \eta_1 + \frac{-c_t - c_s}{m_t} \eta_2 \right) \quad (4.12)$$

taking the time derivative with respect to time,

$$\begin{aligned} \dot{\delta} = & Gw + l\nu - \left( \dot{\eta} + N \left( A_0 X_t + B \left( \alpha^T X + \frac{-k_t - k_s}{m_t} x_t + \frac{-c_t - c_s}{m_t} \dot{x}_t + \nu - \frac{F}{m_t} \right) \right) \right. \\ & \left. + \frac{-\dot{k}_t - \dot{k}_s}{m_t} \dot{\eta}_1 + \frac{-\dot{c}_t - \dot{c}_s}{m_t} \dot{\eta}_2 \right) \end{aligned} \quad (4.13)$$

Substituting (4.11), (4.3), (4.4) and (4.6) into (4.13), considering  $l$  is chosen and  $N = \frac{lB^T}{B^T B}$  where  $N \in \mathbb{R}^{2q \times 2q}$ , we get;

$$\dot{\delta} = Gz - \left( G\xi + G \frac{-k_t - k_s}{m_t} \eta_1 + G \frac{-c_t - c_s}{m_t} \eta_2 \right) \quad (4.14)$$

plugging  $\delta$  into  $\dot{\delta}$ , yields;

$$\dot{\delta} = G\delta \quad (4.15)$$

Keeping in mind that  $G$  is a Hurwitz matrix, we conclude that  $\delta \rightarrow 0$  as  $t \rightarrow \infty$ .  $\square$

Then, plugging (4.10) into the plant (4.1), the following equation is obtained;

$$\dot{X} = A_0 X + B \left( \gamma^T (X - X_t) + \frac{F}{m_s} \right) \quad (4.16)$$

$$\dot{X}_t = A_0 X_t + B \left( \alpha^T X + \mu^T X_t + \theta^T \delta + \theta^T \xi + \beta_1 \eta_1 + \beta_2 \eta_2 - \frac{F}{m_t} \right) \quad (4.17)$$

### 4.3. Controller Design

The model (4.1) is controlled by using an electromagnetic actuator which is placed in between the body and the tire. Our aim is to reduce the effect of the body motion despite the road disturbance. Therefore, the controller  $F$  focuses on the body of the vehicle.

In previous section, the dynamics of the actuator is not taking into account. In this section, the dynamics of the actuator is assumed according to the model which is given in Section 2.40. The force of the actuator depends on current. Thus, a desired controller is based on the current of the actuator.

The backstepping procedure is employed to overcome the unmatched input between the force and the dynamics of the actuator. The current of the actuator is considered as a virtual input which is given as follows;

$$I_d = \frac{1}{K_i \hat{m}_s} \psi \quad (4.18)$$

where  $\psi = KX - \hat{\gamma}^T(X - X_t)$  and  $K \in \mathbb{R}^{2 \times 1}$  is the controller gain matrix.

Using the certainty of equivalence principle, estimations are;

$$\begin{aligned} \tilde{m}_s &= \bar{m}_s - \hat{m}_s \\ \tilde{\gamma}^T &= \gamma^T - \hat{\gamma}^T \\ \tilde{\mu}^T &= \mu^T - \hat{\mu}^T \\ \tilde{\theta}^T &= \theta^T - \hat{\theta}^T \\ \tilde{\beta}_1^T &= \beta_1^T - \hat{\beta}_1^T \\ \tilde{\beta}_2^T &= \beta_2^T - \hat{\beta}_2^T \end{aligned} \quad (4.19)$$

where " $\tilde{\sim}$ " represents the estimation error, " $\hat{\sim}$ " is the estimation term.

The error term between actual input ( $I$ ) and desired input ( $I_d$ ) is;

$$e = I - I_d \quad (4.20)$$

The adaptive controller is given by the following;

$$V = -ce - H(t) \quad (4.21)$$

where  $c > 0$ ,

$$\begin{aligned} H(t) = & \frac{K_i}{L_c} \left( -IR - K_e(\dot{X} - \dot{X}_t) \right) + \frac{\hat{m}_s \psi}{K_i (\hat{m}_s)^2} - \frac{1}{K_i \hat{m}_s} \left( (K - \hat{\gamma}^T) \left( (A_0 + BK)X \right. \right. \\ & \left. \left. + BeK_i \hat{m}_s \right) - \hat{\gamma}^T (X - X_t) - \hat{\gamma}^T (A_0 X + B(\alpha^T X + \hat{\mu}^T X_t + \hat{\theta}^T \xi + \hat{\beta}_1^T \eta_1 \right. \\ & \left. \left. + \hat{\beta}_2^T \eta_2 - \frac{F}{m_t}) \right) \right) + X^T P B k_i \hat{m}_s \end{aligned} \quad (4.22)$$

P is a positive definite matrix which obeys;

$$(A_0 + BK)^T P + P(A_0 + BK) = -2I \quad (4.23)$$

The update laws are;

$$\dot{\hat{\gamma}}^T = (X^T P - \frac{e}{k_i \hat{m}_s} (K - \hat{\gamma}^T)) B (X - X_t) \quad (4.24)$$

$$\dot{\hat{\mu}}^T = \frac{e}{k_i \hat{m}_s} \hat{\gamma}^T B X_t \quad (4.25)$$

$$\dot{\hat{\theta}}^T = \frac{e}{k_i \hat{m}_s} \hat{\gamma}^T B \xi \quad (4.26)$$

$$\dot{\hat{\beta}}_1^T = \frac{e}{k_i \hat{m}_s} \hat{\gamma}^T B \eta_1 \quad (4.27)$$

$$\dot{\hat{\beta}}_2^T = \frac{e}{k_i \hat{m}_s} \hat{\gamma}^T B \eta_2 \quad (4.28)$$

$$\dot{\hat{m}}_s = (X^T P - \frac{e}{k_i \hat{m}_s} (K - \hat{\gamma}^T)) B (e k_i + \frac{\psi}{\hat{m}_s}) \quad (4.29)$$

Since  $\hat{m}_s$  is in the denominator of  $I_d$  (4.18), the projection method is applied to avoid singularity.

$$\dot{\hat{m}}_s = \begin{cases} 0, & \text{If } \hat{m}_s = 0 \text{ and } \dot{\hat{m}}_s < 0 \\ \dot{\hat{m}}_s, & \text{If } \hat{m}_s = 0 \text{ and } \dot{\hat{m}}_s \geq 0 \\ \dot{\hat{m}}_s & \text{Otherwise} \end{cases} \quad (4.30)$$

#### 4.4. Stability

**Theorem 4.2.** *Consider the plant (4.16) with the disturbance observer (3.8), the adaptive controller (4.18). In view of model assumptions,*

- (i) *The equilibrium  $\tilde{m}_s$ ,  $\tilde{\theta}^T$ ,  $\tilde{\beta}_1^T$ ,  $\tilde{\beta}_2^T$ ,  $\tilde{\mu}^T$  and  $\tilde{\gamma}^T$  and  $\tilde{\gamma}^T$  are stable,  $X$ ,  $e$  and  $\delta$  converge to zero while time goes to  $\infty$ .*
- (ii) *The signal  $I$  is bounded for all initial conditions.*

*Proof.* In equation (4.16), there are unknown terms which cannot be used in Lyapunov function. However, if the plant is represented in terms of estimations and error functions with considering the certainty of equivalence principle, they can be used in Lyapunov function. The application of this representation is given as follows;

Plugging (4.18) into (4.16) and (4.21) into the time derivative of (4.20), the following system is obtained;

$$\begin{aligned} \dot{X} &= (A_0 + BK)X + B \left( \tilde{\gamma}^T (X - X_t) + \tilde{m}_s (ek_i + \frac{\psi}{\hat{m}_s}) \right) \\ \dot{X}_t &= A_0 X_t + B \left( \alpha^T X + (\tilde{\mu}^T + \hat{\mu}^T) X_t + \theta^T \delta + (\tilde{\theta}^T + \hat{\theta}^T) \xi + (\tilde{\beta}_1 + \hat{\beta}_1) \eta_1 \right. \\ &\quad \left. + (\tilde{\beta}_2 + \hat{\beta}_2) \eta_2 - \frac{F}{m_t} \right) \end{aligned} \quad (4.31)$$

$$\begin{aligned} \dot{e} = & -ce - \frac{1}{k_i \hat{m}_s} \left( (K - \hat{\gamma}^T) B \left( \hat{\gamma}^T (X - X_t) + ek_i \tilde{m}_s + \frac{\tilde{m}_s}{\hat{m}_s} \right) \right. \\ & \left. - \hat{\gamma}^T B \left( \tilde{\mu}^T X_t + \theta^T \delta + \tilde{\theta}^T \xi + \tilde{\beta}_1^T \eta_1 + \tilde{\beta}_2^T \eta_2 - \frac{F}{m_t} \right) \right) \end{aligned} \quad (4.32)$$

Choosing the following Lyapunov function, the stability of the closed loop system is established;

$$V = \frac{1}{2} \left( X^T P X + e^2 + \frac{\tilde{m}_s^2}{\alpha_{m_s}} + \frac{\tilde{\gamma}^T \tilde{\gamma}}{\alpha_\gamma} + \frac{\tilde{\mu}^T \tilde{\mu}}{\alpha_\mu} + \frac{\tilde{\theta}^T \tilde{\theta}}{\alpha_\mu} + \frac{\tilde{\beta}_1^T \tilde{\beta}_1}{\alpha_\mu} + \frac{\tilde{\beta}_2^T \tilde{\beta}_2}{\alpha_\mu} + \delta^T P_G \delta \right) \quad (4.33)$$

where  $G^T P_G + P_G G = -2\epsilon I$

Deriving V with respect to time,

$$\begin{aligned} \dot{V} = & \frac{1}{2} \left( X^T P \dot{X} + 2e\dot{e} - 2\frac{\tilde{m}_s \dot{\tilde{m}}_s}{\alpha_{m_s}} - 2\frac{\tilde{\gamma}^T \dot{\tilde{\gamma}}}{\alpha_\gamma} - 2\frac{\tilde{\mu}^T \dot{\tilde{\mu}}}{\alpha_\mu} - 2\frac{\tilde{\theta}^T \dot{\tilde{\theta}}}{\alpha_\theta} - 2\frac{\tilde{\beta}_1^T \dot{\tilde{\beta}}_1}{\alpha_{\beta_1}} \right. \\ & \left. - 2\frac{\tilde{\beta}_2^T \dot{\tilde{\beta}}_2}{\alpha_{\beta_2}} + \delta^T P_G \dot{\delta} \right) \end{aligned} \quad (4.34)$$

Substituting (4.24), (4.31) and (4.32) into (4.34), we get;

$$\dot{V} = X^T P (A_0 + BK) X + X^T (A_0 + BK)^T P X - ce^2 + \frac{e}{k_i \hat{m}_s} \hat{\gamma}^T B \theta^T \delta - \epsilon \delta^T \delta \quad (4.35)$$

In order to handle the cross term, Young's Inequality is applied in the following [13].

$$\frac{e}{k_i \hat{m}_s} \hat{\gamma}^T B \theta^T \delta \leq \frac{e^2}{2(k_i \hat{m}_s)^2} + \frac{\delta^T \theta B^T \hat{\gamma} \hat{\gamma}^T B \theta^T \delta}{2} \quad (4.36)$$

$$\frac{e}{k_i \hat{m}_s} \hat{\gamma}^T B \theta^T \delta \leq \frac{1}{2(k_i \hat{m}_s)^2} e^2 + \lambda_{max}(\theta B^T \hat{\gamma} \hat{\gamma}^T B \theta^T) \delta^T \delta \quad (4.37)$$

If we choose  $c = 1 + \frac{1}{2(k_i \hat{m}_s)^2}$ ,  $\epsilon = 1 + \lambda_{max}(\theta B^T \hat{\gamma} \hat{\gamma}^T B \theta^T)$  and considering (4.23), we get;

$$\dot{V} \leq -X^T X - e^2 - \delta^T \delta \quad (4.38)$$

then, it is concluded

$$V(t) \leq V(0) \quad (4.39)$$

which implies that  $V(t)$  is bounded. Define;

$$\varsigma = \begin{bmatrix} X & e & \tilde{\gamma}^T & \tilde{m}_s & \tilde{\mu}^T & \tilde{\theta}^T & \tilde{\beta}_1^T & \tilde{\beta}_2^T & \delta \end{bmatrix} \quad (4.40)$$

Considering (4.33) and (4.39), the following function is obtained;

$$|\varsigma|^2 \leq M_1 |\varsigma(0)|^2 \quad (4.41)$$

where  $M_1 > 0$ .  $\forall \varsigma$ , the right hand side of (4.15), (4.19), (4.24) and (4.31) are continuous in  $\varsigma$  and time, which tells us that the right hand side of (4.38) is continuous in  $\varsigma$  and time. Moreover, the right hand side of (4.38) is zero when  $\varsigma = 0$ . By using Lasalle-Yoshisawa theorem [13], (4.38) assures that  $X$ ,  $e$  and  $\delta$  converge to zero while time goes to  $\infty$ . Since,  $\tilde{\gamma}^T$ ,  $\tilde{m}_s$ ,  $\tilde{\mu}^T$ ,  $\tilde{\theta}^T$ ,  $\tilde{\beta}_1^T$  and  $\tilde{\beta}_2^T$  are bounded, it follows that  $\hat{\gamma}^T$ ,  $\hat{m}_s$ ,  $\hat{\mu}^T$ ,  $\hat{\theta}^T$ ,  $\hat{\beta}_1^T$  and  $\hat{\beta}_2^T$  are bounded considering (4.19). Furthermore, in the light of the boundedness of the suspension gap  $(X - X_t)$  and  $X$ , it is concluded that  $X_t$  and  $\dot{X}_t$  are bounded.

Since the disturbance consists of a sum of sinusoidal (2.42),  $\nu$  is bounded. Considering  $G$  is Hurwitz, it is concluded that  $\delta$  is bounded from (4.15). With using (4.11), we can say that  $\xi$ ,  $\eta_1$  and  $\eta_2$  are bounded which leads to the boundedness of  $\theta$ ,  $\beta_1$  and  $\beta_2$  with considering (4.10). Since  $\bar{m}_s$ ,  $\gamma^T$  and  $\mu^T$  are constant values and  $\tilde{m}_s$ ,  $\tilde{\gamma}^T$ ,  $\tilde{\gamma}^T$ ,  $\tilde{\theta}^T$ ,  $\tilde{\beta}_1^T$ ,  $\tilde{\beta}_2^T$ ,  $\theta$ ,  $\beta_1$  and  $\beta_2$  are bounded, it is attained that the estimations  $(\hat{\gamma}^T, \hat{m}_s, \hat{\mu}^T, \hat{\theta}^T, \hat{\beta}_1^T$  and  $\hat{\beta}_2^T)$  are bounded. Moreover, bearing in mind the fact that  $K$  is a negative definite matrix,  $X$ ,  $\dot{X}$ , the estimations are bounded, it is concluded that  $I_d$  is bounded with using (4.18). Then, with using (4.20), it is attained that  $I$  is bounded.  $\square$

### 4.5. Simulation

In this part, the effectiveness of the proposed controller for the quarter car model is demonstrated. To represent the disturbance input, a sum of sinusoidal is given by;

$$\nu = \begin{cases} 0 & 0 \leq t \leq 4 \\ \nu_{d1} & 4 < t \leq 10 \\ 0 & 10 < t \leq 11 \\ \nu_{d2} & 11 < t \leq 18 \\ 0 & 18 < t \leq 20 \end{cases} \quad (4.42)$$

where;

$$\begin{aligned} \nu_{d1} &= 0.03 \sin\left(2\pi t + \frac{\pi}{8}\right) + 0.01 \sin(5\pi t) \\ \nu_{d2} &= 0.02 \sin(15\pi t) + 0.03 \sin\left(18\pi t + \frac{\pi}{4}\right) \end{aligned} \quad (4.43)$$

Two different road profile is applied to the vehicle. Here,  $\nu_{d1}$  represents low frequency range,  $\nu_{d2}$  represents the high frequency range.

The parameters of the plant is taken from Appendix B. Initial conditions for all states are chosen as zero except the singular term which is chosen as  $\hat{m} = 54$ . Figure 4.1 displays the displacement response of the vehicle body in time domain for 20 seconds. The acceleration of the body is depicted in Figure 4.2. The vehicle is exposed the road disturbance as stated 5.43. The simulation results demonstrate that the active suspension (Closed Loop Response) demonstrates much better performance than the passive suspension system (Open Loop). Since the effect of the road roughness is not transmitted to the vehicle body, perceived comfort by passengers is improved by using active suspension system.

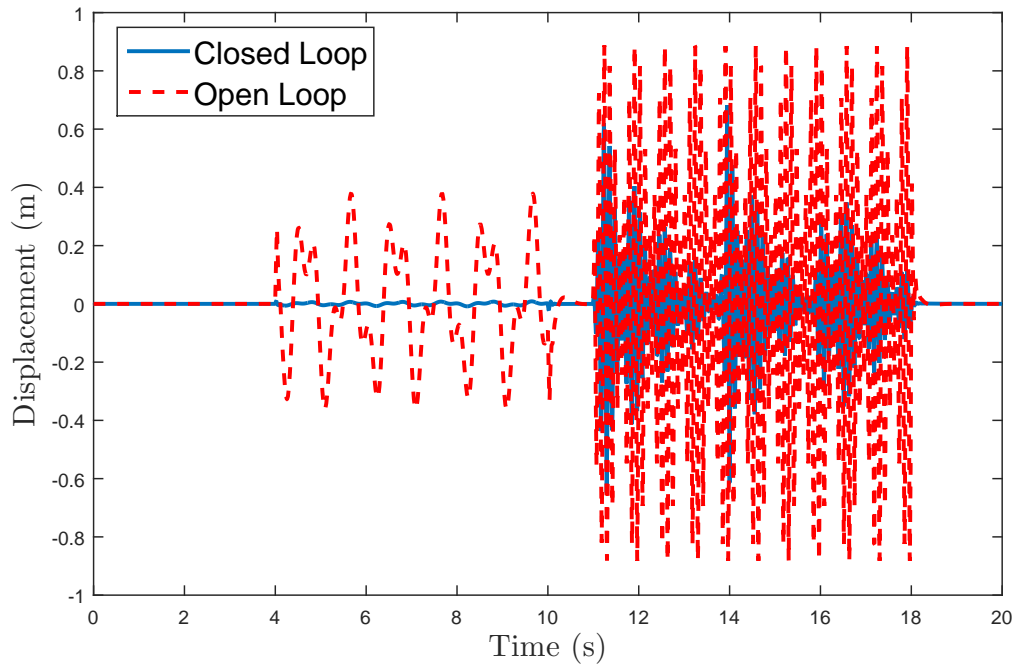


Figure 4.1. The displacement response of the body.

Figure 4.3 and 4.4 illustrate a comparison between the adaptive controller and LQR for the displacement and acceleration responses of the body, respectively. To compare the performance of the controllers, the disturbance input is given in 3.43. The parameters for LQR controller are chosen as  $R = 0.000001$  and  $Q = \begin{bmatrix} 35 & 0 & 0 & 0 \\ 0 & 45 & 0 & 0 \\ 0 & 0 & 55 & 0 \\ 0 & 0 & 0 & 65 \end{bmatrix}$  the Although the assumptions, which are the parametric uncertainty, the dynamics of the actuator and unmeasured disturbance, are not taken into consideration, it is clear that the adaptive controller is improved the ride comfort much better than the LQR. Moreover, even though LQR attenuates the disturbance input, the adaptive controller offers the cancellation of the disturbance.

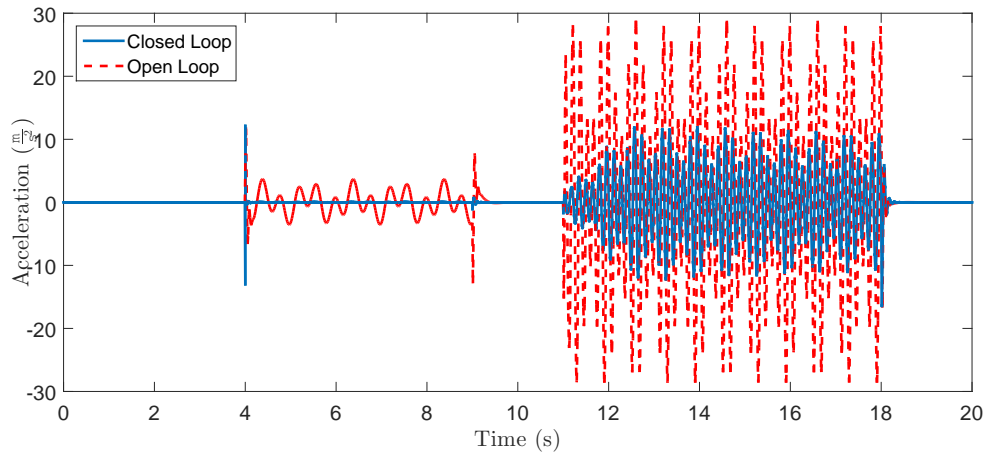


Figure 4.2. The acceleration response of the body.

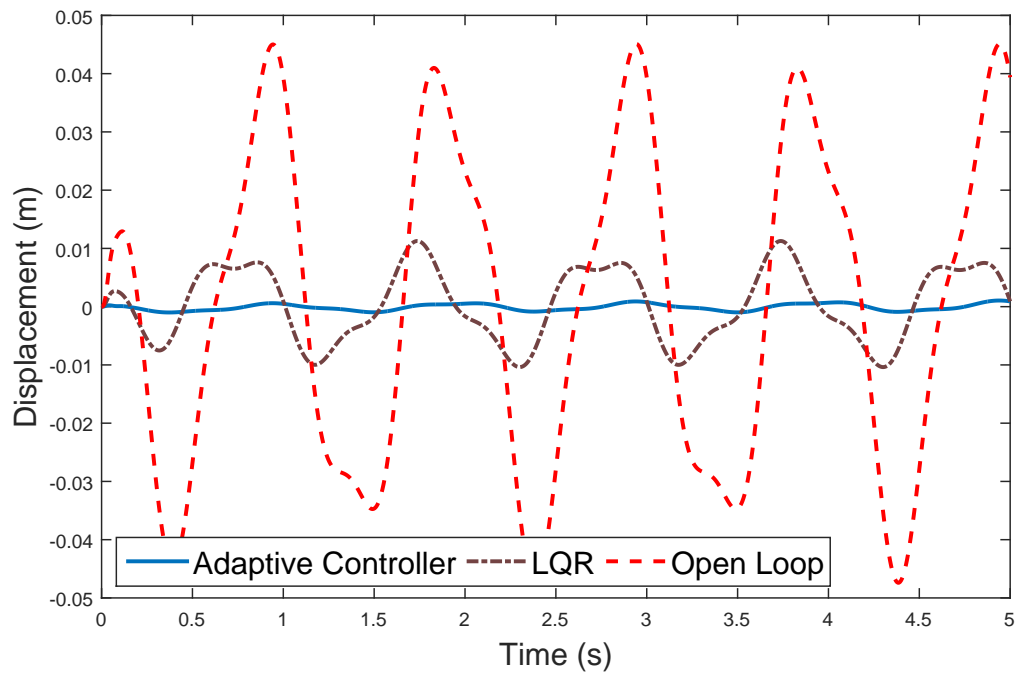


Figure 4.3. Comparison between the adaptive controller and LQR for the displacement response of the body.

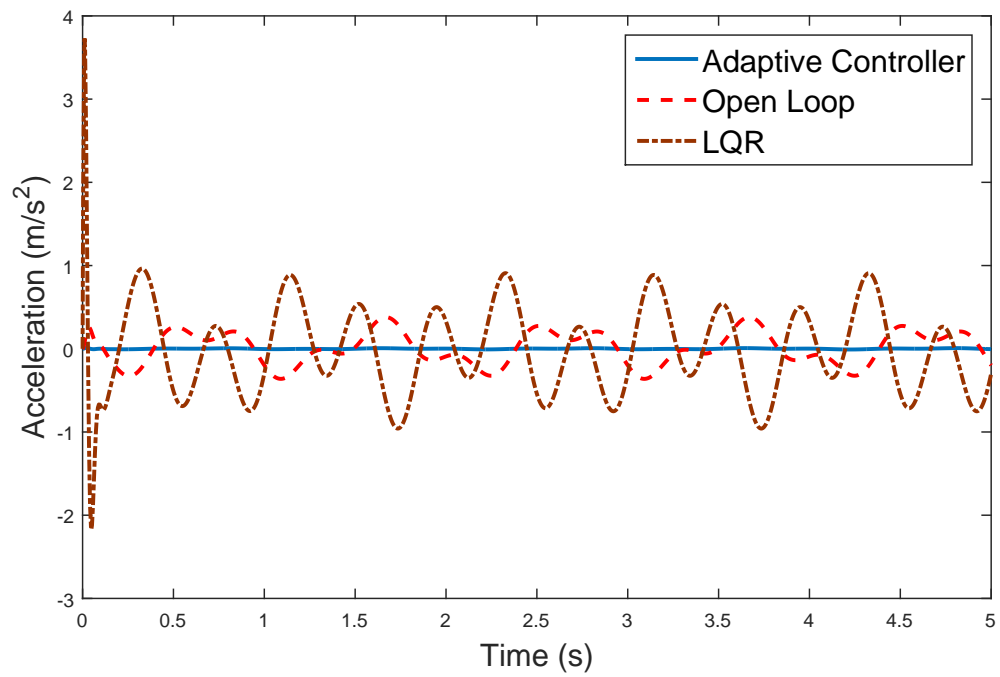


Figure 4.4. Comparison between the adaptive controller and LQR for the acceleration response of the body.

## **5. DESIGN OF AN ADAPTIVE BACKSTEPPING CONTROLLER FOR A HALF CAR MODEL WITH CONSIDERING PARAMETRIC UNCERTAINTY**

In this chapter, the design of an adaptive backstepping controller for a half car model is discussed. The model contains two actuator which their duties are to control the vertical acceleration and the body pitch of a vehicle. The parametric uncertainty of tire and body mass is taken into account same as Chapter 4. In addition, inertia of the body and actuator terms are considered as unknown.

To reduce the implementation cost, it is assumed that the vertical velocity of the body, the velocity and displacement of the tire and the relative motion between the tire and the body is only available for measurement. Moreover, the road disturbance is not measured same as previous chapter. However, there are two different road inputs that affect the body at the same time. Therefore, observers are designed for a front and a rear disturbance input, respectively.

Since partial states are available for measurement, an adaptive backstepping controller is designed by considering these states. Lyapunov approach is used to establish asymptotically stability of the plant.

### **5.1. Problem Statement**

The derivation of the half car model is given in equation (2.39). The half car model is equipped with two actuators. It is assumed that the dynamics of them are identical.

The front actuator dynamics is given as follows;

$$\begin{aligned} F_f &= K_i I_1 \\ \dot{I}_1 &= AV_1 - BI_1 - C\dot{x}_{su}^f \end{aligned} \quad (5.1)$$

The rear actuator dynamics is given as follows;

$$\begin{aligned} F_r &= K_i I_2 \\ \dot{I}_2 &= AV_2 - BI_2 - C\dot{x}_{su}^r \end{aligned} \quad (5.2)$$

where  $A = \frac{1}{L_c}$ ,  $B = \frac{R}{L_c}$  and  $C = \frac{K_e}{L_c}$ .

Let us recall that the dynamics of the plant which derived in Section 2.2

$$\begin{aligned} \ddot{x}_b &= a_1(x_{su}^f) + a_{n1}(x_{su}^f)^3 + a_2(x_{su}^r) + a_{n2}(x_{su}^r)^3 + a_3(\dot{x}_{su}^f) + a_4(\dot{x}_{su}^r) + \bar{m}_b U_1 \\ \ddot{\varrho} &= b_1(x_{su}^f) + b_{n1}(x_{su}^f)^3 + b_2(x_{su}^r) + b_{n2}(x_{su}^r)^3 + b_3(\dot{x}_{su}^f) + b_4(\dot{x}_{su}^r) + \bar{I}_b U_2 \\ \ddot{x}_t^f &= c_1(x_{su}^f) + c_{n1}(x_{su}^f)^3 + c_2 \dot{x}_t^f + c_3(x_{su}^f) + c_4 \dot{x}_t^f + \nu_1 - \frac{F_f}{m_t^f} \\ \ddot{x}_t^r &= d_1(x_{su}^r) + d_{n1}(x_{su}^r)^3 + d_2 \dot{x}_t^r + d_3(x_{su}^r) + d_4 \dot{x}_t^r + \nu_2 - \frac{F_r}{m_t^r} \end{aligned} \quad (5.3)$$

### 5.1.1. Model Assumptions

- Partial states, which are the vertical velocity of the body, the vertical displacement and velocity of the tire and suspension stroke are measured.
- The inertia and the mass of the body, the parameters of the tire and actuators are considered as unknown.
- The relative displacements between the body ( $X_b$ ) and the front and the rear tire ( $X_t^f$  and  $X_t^r$ ) are limited within the suspension gap.

## 5.2. Road Disturbance Representation

The front and rear tire are represented in the half car model. Therefore, the body is exposed to different disturbances at the same time. In this part, observers are designed for both tire, separately.

**Lemma 5.1.** *The observer for the front tire;*

$$\nu_1 = \theta_1^T \delta_1 + \theta_1^T \xi_{11} + \beta_1^T \eta_1 + \beta_2^T \eta_2 \quad (5.4)$$

and for the rear tire;

$$\nu_2 = \theta_2^T \delta_2 + \theta_2^T \xi_{22} + \beta_3^T \eta_3 + \beta_4^T \eta_4 \quad (5.5)$$

where  $\beta_1^T = c_2 \theta_1^T$ ,  $\beta_2^T = c_4 \theta_1^T$ ,  $\beta_3^T = d_2 \theta_2^T$  and  $\beta_4^T = d_4 \theta_2^T$ .

The filters are given for the front and the rear tire, respectively.

$$\begin{aligned} \xi_{11} &= \eta_{11} + l \dot{x}_t^f \\ \dot{\eta}_{11} &= G \xi_{11} - l \left( c_1 x_{su}^f + c_{1n} (x_{su}^f)^3 + c_3 \dot{x}_{su}^f - \frac{F_f}{m_f} \right) \\ \dot{\eta}_1 &= G \eta_1 - l x_t^f \\ \dot{\eta}_2 &= G \eta_2 - l \dot{x}_t^f \\ \xi_{22} &= \eta_{22} + l \dot{x}_t^r \\ \dot{\eta}_{22} &= G \xi_{22} - l \left( d_1 x_{su}^r + d_{1n} (x_{su}^r)^3 + d_3 \dot{x}_{su}^r - \frac{F_r}{m_r} \right) \\ \dot{\eta}_3 &= G \eta_3 - l x_t^r \\ \dot{\eta}_4 &= G \eta_4 - l \dot{x}_t^r \end{aligned} \quad (5.6)$$

obeys;

$$\begin{aligned} \dot{\delta}_1 &= G \delta_1 \\ \dot{\delta}_2 &= G \delta_2 \end{aligned} \quad (5.7)$$

*Proof.* Estimation errors can be defined as;

$$\begin{aligned}\delta_1 &= w_1 - \left( \xi_{11} + c_2\eta_1 + c_4\eta_2 \right) \\ \delta_2 &= w_2 - \left( \xi_{22} + d_2\eta_3 + d_4\eta_4 \right)\end{aligned}\tag{5.8}$$

taking the derivative of errors with respect to time;

$$\begin{aligned}\dot{\delta}_1 &= \dot{w}_1 - \left( \dot{\xi}_{11} + c_2\dot{\eta}_1 + c_4\dot{\eta}_2 \right) \\ \dot{\delta}_2 &= \dot{w}_2 - \left( \dot{\xi}_{22} + d_2\dot{\eta}_3 + d_4\dot{\eta}_4 \right)\end{aligned}\tag{5.9}$$

Because of the fact that the plant have two actuators, equation (2.47) is converted to our case. Here, Subscript 1 denotes the front tire, subscript 2 denotes the rear tire.

$$\begin{aligned}\dot{z}_1 &= Gw_1 + l\nu_1 \\ \dot{z}_2 &= Gw_2 + l\nu_2\end{aligned}\tag{5.10}$$

Then, substituting (5.6) and (5.10) into (5.9), the following is obtained;

$$\begin{aligned}\dot{\delta}_1 &= G\left( w_1 - (\xi_{11} + c_2\eta_1 + c_4\eta_2) \right) \\ \dot{\delta}_2 &= G\left( w_2 - (\xi_{22} + d_2\eta_3 + d_4\eta_4) \right)\end{aligned}\tag{5.11}$$

Considering (5.8), obeys

$$\begin{aligned}\dot{\delta}_1 &= G\delta_1 \\ \dot{\delta}_2 &= G\delta_2\end{aligned}\tag{5.12}$$

We conclude that  $\delta_1 \rightarrow 0$  and  $\delta_2 \rightarrow 0$  as time goes to 0. □

Plugging (5.4) and (5.5) into the plant (2.39), we obtain;

$$\begin{aligned}
\ddot{x}_b &= a_1 x_{su}^f + a_{1n} (x_{su}^f)^3 + a_2 x_{su}^r + a_{2n} (x_{su}^r)^3 + a_3 \dot{x}_{su}^f + a_4 \dot{x}_{su}^r + \bar{m}_b U_1 \\
\ddot{\theta} &= b_1 x_{su}^f + b_{1n} (x_{su}^f)^3 + b_2 x_{su}^r + b_{2n} (x_{su}^r)^3 + b_3 \dot{x}_{su}^f + b_4 \dot{x}_{su}^r + \bar{I}_b U_2 \\
\ddot{x}_t^f &= c_1 x_{su}^f + c_{1n} (x_{su}^f)^3 + c_2 x_t^f + c_3 \dot{x}_{su}^f + c_4 \dot{x}_t^f + \theta_1^T \delta_1 + \theta_1^T \xi_1 + \beta_1^T \eta_1 + \beta_2^T \eta_2 - \frac{F_f}{m_t^f} \\
\ddot{x}_t^r &= d_1 x_{su}^r + d_{1n} (x_{su}^r)^3 + d_2 x_t^r + d_3 \dot{x}_{su}^r + d_4 \dot{x}_t^r + \theta_2^T \delta_2 + \theta_2^T \xi_2 + \beta_3^T \eta_3 + \beta_4^T \eta_4 - \frac{F_r}{m_t^r}
\end{aligned} \tag{5.13}$$

### 5.3. Controller Design

In the half car model, there are two motions that affect the comfort of passengers and the performance of the vehicle. These are heave and pitch motions. Since actuator dynamics is considered, the unmatched input is encountered same as Chapter 4. To handle this problem, the backstepping procedure is employed.

To regulate the motion of the body, the following desired inputs in other word, virtual controllers are offered.  $U_1$ , which is given in (5.14), is designed to control the heave motion of vehicle.

$$U_{1d} = \frac{1}{\hat{m}_b} (\psi_1) \tag{5.14}$$

To control the pitch motion of the car,  $U_2$  is designed in (5.15).

$$U_{2d} = \frac{1}{\hat{I}_b} (\psi_2) \tag{5.15}$$

$\psi_1$  and  $\psi_1$  are defined as;

$$\psi_1 = \kappa_1 \dot{x}_b - \hat{a}_1 x_{su}^f - \hat{a}_{1n} (x_{su}^f)^3 - \hat{a}_2 x_{su}^r - \hat{a}_{2n} (x_{su}^r)^3 - \hat{a}_3 \dot{x}_{su}^f - \hat{a}_4 \dot{x}_{su}^r \quad (5.16)$$

$$\psi_2 = \kappa_2 \dot{q} - \hat{b}_1 x_{su}^f - \hat{b}_{1n} (x_{su}^f)^3 - \hat{b}_2 x_{su}^r - \hat{b}_{2n} (x_{su}^r)^3 - \hat{b}_3 \dot{x}_{su}^f - \hat{b}_4 \dot{x}_{su}^r \quad (5.17)$$

where,  $\kappa_1 < 0$ ,  $\kappa_2 < 0$ .

In view of the certainty of equivalence principle, estimations for the unknown terms are;

$$\begin{aligned} \tilde{a}_1 &= a_1 - \hat{a}_1 & \tilde{b}_1 &= b_1 - \hat{b}_1 & \tilde{c}_2 &= c_2 - \hat{c}_2 \\ \tilde{a}_2 &= a_2 - \hat{a}_2 & \tilde{b}_2 &= b_2 - \hat{b}_2 & \tilde{c}_4 &= c_4 - \hat{c}_4 \\ \tilde{a}_{1n} &= a_{1n} - \hat{a}_{1n} & \tilde{b}_{1n} &= b_{1n} - \hat{b}_{1n} & \tilde{d}_2 &= d_2 - \hat{d}_2 \\ \tilde{a}_{2n} &= a_{2n} - \hat{a}_{2n} & \tilde{b}_{2n} &= b_{2n} - \hat{b}_{2n} & \tilde{d}_4 &= d_4 - \hat{d}_4 \\ \tilde{a}_3 &= a_3 - \hat{a}_3 & \tilde{b}_3 &= b_3 - \hat{b}_3 & \tilde{m} &= \bar{m} - \hat{m} \\ \tilde{a}_4 &= a_4 - \hat{a}_4 & \tilde{b}_4 &= b_4 - \hat{b}_4 & \tilde{I}_n &= \bar{I}_n - \hat{I}_n \\ \tilde{\theta}_1^T &= \theta_1^T - \hat{\theta}_1^T & \tilde{\beta}_1^T &= \beta_1^T - \hat{\beta}_1^T & \tilde{\beta}_2^T &= \beta_2^T - \hat{\beta}_2^T \\ \tilde{\theta}_2^T &= \theta_2^T - \hat{\theta}_2^T & \tilde{\beta}_3^T &= \beta_3^T - \hat{\beta}_3^T & \tilde{\beta}_4^T &= \beta_4^T - \hat{\beta}_4^T \\ \tilde{A} &= A - \hat{A} & \tilde{B} &= B - \hat{B} & \tilde{C} &= C - \hat{C} \end{aligned} \quad (5.18)$$

The error terms for  $U_1$  and  $U_2$  are;

$$\begin{aligned} e_1 &= U_1 - U_{1d} \\ e_2 &= U_2 - U_{2d} \end{aligned} \quad (5.19)$$

In view of equations (5.1), (5.2) and (5.13), taking the derivative of error terms with respect to time yields;

$$\begin{aligned} \dot{e}_1 = & (\tilde{A} + \hat{A})(V_1 + V_2) - (\tilde{A} + \hat{A})(\tilde{R} + \hat{R})(I_1 + I_2) - (\tilde{k}_e + \hat{k}_e)(\dot{x}_{su}^f + \dot{x}_{su}^r) \\ & - \left( \frac{\dot{\psi}_1 \hat{m}_b - \dot{\hat{m}}_b \psi_1}{(\hat{m}_b)^2} \right) \end{aligned} \quad (5.20)$$

$$\begin{aligned} \dot{e}_2 = & (\tilde{A} + \hat{A})(-aV_1 + bV_2) - (\tilde{A} + \hat{A})(\tilde{R} + \hat{R})(-aI_1 + bI_2) \\ & - (\tilde{k}_e + \hat{k}_e)(-a\dot{x}_{su}^f + b\dot{x}_{su}^r) - \left( \frac{\dot{\psi}_2 \hat{I}_b - \dot{\hat{I}}_b \psi_2}{(\hat{I}_b)^2} \right) \end{aligned} \quad (5.21)$$

the inputs for the both error function are chosen as;

$$\begin{aligned} V_1 + V_2 &= \frac{1}{\hat{A}}(-c_1 e_1 - H_1) \\ -aV_1 + bV_2 &= \frac{1}{\hat{A}}(-c_2 e_1 - H_2) \end{aligned} \quad (5.22)$$

where  $c_1 > 0$  and  $c_2 > 0$ . Solving (5.22) with using the method of elimination, the adaptive controllers are obtained as;

$$\begin{aligned} V_1 &= \frac{1}{\hat{A}} \left( \frac{-bc_1 e_1 - bH_1 + c_2 e_2 + H_2}{a + b} \right) \\ V_2 &= \frac{1}{\hat{A}} \left( \frac{-ac_1 e_1 - aH_1 - c_2 e_2 - H_2}{a + b} \right) \end{aligned} \quad (5.23)$$

where;

$$\begin{aligned}
H_1 = & \hat{m}_b \dot{x}_b - \hat{B}(I_1 + I_2) - \hat{C}(\dot{x}_{su}^f + \dot{x}_{su}^r) + \frac{\dot{\hat{m}}_b \psi_1}{(\hat{m}_b)^2} - \frac{1}{\hat{m}_b} \left( -\dot{\hat{a}}_1 x_{su}^f - \dot{\hat{a}}_{1n} (x_{su}^f)^3 \right. \\
& - \dot{\hat{a}}_2 x_{su}^r - \dot{\hat{a}}_{2n} (x_{su}^r)^3 + (-\dot{\hat{a}}_3 - 3\dot{\hat{a}}_{1n} (x_{su}^f)^2 - \dot{\hat{a}}_1) \dot{x}_{su}^f \\
& + (-\dot{\hat{a}}_4 - \dot{\hat{a}}_2 - 3\dot{\hat{a}}_{2n} (x_{su}^r)^2) \dot{x}_{su}^r + (\kappa_1 - \dot{\hat{a}}_3 - \dot{\hat{a}}_4) (\kappa_1 \dot{x}_b + \hat{m}_b e_1) \\
& + (a\dot{\hat{a}}_3 - b\dot{\hat{a}}_4) (\kappa_2 \dot{\varrho} + \hat{I}_b e_2) \\
& + \hat{a}_3 \left( c_1 x_{su}^f + c_{1n} (x_{su}^f)^3 + \hat{c}_2 x_t^f + c_3 \dot{x}_{su}^f + \hat{c}_4 (\dot{x}_t^f) + \hat{\theta}_1^T \xi_{11} + \hat{\beta}_1^T \eta_1 + \hat{\beta}_2^T \eta_2 - \frac{F_f}{m_t^f} \right) \\
& \left. + \hat{a}_4 \left( d_1 x_{su}^r + d_{1n} (x_{su}^r)^3 + \hat{d}_2 x_t^r + d_3 \dot{x}_{su}^r + \hat{d}_4 (\dot{x}_t^r) + \hat{\theta}_2^T \xi_{22} + \hat{\beta}_3^T \eta_3 + \hat{\beta}_4^T \eta_4 - \frac{F_r}{m_t^r} \right) \right)
\end{aligned} \tag{5.24}$$

$$\begin{aligned}
H_2 = & \hat{I}_b \dot{\varrho} + \hat{B}(-aI_1 + bI_2) + \hat{C}(-a\dot{x}_{su}^f + b\dot{x}_{su}^r) + \frac{\dot{\hat{I}}_b \psi_2}{(\hat{I}_b)^2} - \frac{1}{\hat{I}_b} \left( -\dot{\hat{b}}_1 x_{su}^f - \dot{\hat{b}}_{1n} (x_{su}^f)^3 \right. \\
& - \dot{\hat{b}}_2 x_{su}^r - \dot{\hat{b}}_{2n} (x_{su}^r)^3 + (-\dot{\hat{b}}_3 - 3\dot{\hat{b}}_{1n} (x_{su}^f)^2 - \dot{\hat{b}}_1) \dot{x}_{su}^f \\
& + (-\dot{\hat{b}}_4 - \dot{\hat{b}}_2 \dot{x}_{su}^r - 3\dot{\hat{b}}_{2n} (x_{su}^r)^2) \dot{x}_{su}^r + (\kappa_2 - a\dot{\hat{b}}_3 + b\dot{\hat{b}}_4) (\kappa_2 \dot{\varrho} + \hat{I}_b e_2) \\
& + (-\dot{\hat{b}}_3 - \dot{\hat{b}}_4) (\kappa_1 \dot{x}_b + \hat{m}_b e_1) \\
& + \hat{b}_3 \left( c_1 x_{su}^f + c_{1n} (x_{su}^f)^3 + \hat{c}_2 x_t^f + c_3 \dot{x}_{su}^f + \hat{c}_4 (\dot{x}_t^f) + \hat{\theta}_1^T \xi_{11} + \hat{\beta}_1^T \eta_1 + \hat{\beta}_2^T \eta_2 - \frac{F_f}{m_t^f} \right) \\
& + \hat{b}_4 \left( d_1 x_{su}^r + d_{1n} (x_{su}^r)^3 + \hat{d}_2 x_t^r + d_3 \dot{x}_{su}^r + \hat{d}_4 (\dot{x}_t^r) + \hat{\theta}_2^T \xi_{22} + \hat{\beta}_3^T \eta_3 + \hat{\beta}_4^T \eta_4 \right. \\
& \left. - \frac{F_r}{m_t^r} \right)
\end{aligned} \tag{5.25}$$

The update laws are as follows;

$$\begin{aligned}
\dot{\hat{a}}_1 &= \gamma_{a1} \left( \dot{x}_b - \frac{e_1}{\hat{m}_b} (\kappa_1 - \hat{a}_3 - \hat{a}_4) - \frac{e_2}{\hat{I}_b} (-\hat{b}_3 - \hat{b}_4) \right) (x_{su}^f) \\
\dot{\hat{a}}_2 &= \gamma_{a2} \left( \dot{x}_b - \frac{e_1}{\hat{m}_b} (\kappa_1 - \hat{a}_3 - \hat{a}_4) - \frac{e_2}{\hat{I}_b} (-\hat{b}_3 - \hat{b}_4) \right) (x_{su}^r) \\
\dot{\hat{a}}_3 &= \gamma_{a3} \left( \dot{x}_b - \frac{e_1}{\hat{m}_b} (\kappa_1 - \hat{a}_3 - \hat{a}_4) - \frac{e_2}{\hat{I}_b} (-\hat{b}_3 - \hat{b}_4) \right) (x_{su}^f) \\
\dot{\hat{a}}_4 &= \gamma_{a4} \left( \dot{x}_b - \frac{e_1}{\hat{m}_b} (\kappa_1 - \hat{a}_3 - \hat{a}_4) - \frac{e_2}{\hat{I}_b} (-\hat{b}_3 - \hat{b}_4) \right) (x_{su}^r) \\
\dot{\hat{a}}_{1n} &= \gamma_{a1n} \left( \dot{x}_b - \frac{e_1}{\hat{m}_b} (\kappa_1 - \hat{a}_3 - \hat{a}_4) - \frac{e_2}{\hat{I}_b} (-\hat{b}_3 - \hat{b}_4) \right) (x_{su}^f)^3 \\
\dot{\hat{a}}_{2n} &= \gamma_{a1n} \left( \dot{x}_b - \frac{e_1}{\hat{m}_b} (\kappa_1 - \hat{a}_3 - \hat{a}_4) - \frac{e_2}{\hat{I}_b} (-\hat{b}_3 - \hat{b}_4) \right) (x_{su}^r)^3 \\
\dot{\hat{b}}_1 &= \gamma_{b1} \left( \dot{\rho} - \frac{e_1}{\hat{m}_b} (-a\hat{a}_3 + b\hat{a}_4) - \frac{e_2}{\hat{I}_b} (\kappa_2 - a\hat{b}_3 + b\hat{b}_4) \right) (x_{su}^f) \\
\dot{\hat{b}}_2 &= \gamma_{b2} \left( \dot{\rho} - \frac{e_1}{\hat{m}_b} (-a\hat{a}_3 + b\hat{a}_4) - \frac{e_2}{\hat{I}_b} (\kappa_2 - a\hat{b}_3 + b\hat{b}_4) \right) (x_{su}^r) \\
\dot{\hat{b}}_3 &= \gamma_{b3} \left( \dot{\rho} - \frac{e_1}{\hat{m}_b} (-a\hat{a}_3 + b\hat{a}_4) - \frac{e_2}{\hat{I}_b} (\kappa_2 - a\hat{b}_3 + b\hat{b}_4) \right) (x_{su}^f) \\
\dot{\hat{b}}_4 &= \gamma_{b4} \left( \dot{\rho} - \frac{e_1}{\hat{m}_b} (-a\hat{a}_3 + b\hat{a}_4) - \frac{e_2}{\hat{I}_b} (\kappa_2 - a\hat{b}_3 + b\hat{b}_4) \right) (x_{su}^r) \\
\dot{\hat{b}}_{1n} &= \gamma_{b1n} \left( \dot{\rho} - \frac{e_1}{\hat{m}_b} (-a\hat{a}_3 + b\hat{a}_4) - \frac{e_2}{\hat{I}_b} (\kappa_2 - a\hat{b}_3 + b\hat{b}_4) \right) (x_{su}^f)^3 \\
\dot{\hat{b}}_{2n} &= \gamma_{b2n} \left( \dot{\rho} - \frac{e_1}{\hat{m}_b} (-a\hat{a}_3 + b\hat{a}_4) - \frac{e_2}{\hat{I}_b} (\kappa_2 - a\hat{b}_3 + b\hat{b}_4) \right) (x_{su}^f)^3 \\
\dot{\hat{c}}_2 &= \gamma_{c2} \left( -\frac{e_1}{\hat{m}_b} \hat{a}_3 - \frac{e_2}{\hat{I}_b} \hat{b}_3 \right) (x_t^f) \\
\dot{\hat{c}}_4 &= \gamma_{c4} \left( -\frac{e_1}{\hat{m}_b} \hat{a}_3 - \frac{e_2}{\hat{I}_b} \hat{b}_3 \right) (x_t^f) \\
\dot{\hat{d}}_2 &= \gamma_{d2} \left( -\frac{e_1}{\hat{m}_b} \hat{a}_4 - \frac{e_2}{\hat{I}_b} \hat{b}_4 \right) (x_t^r) \\
\dot{\hat{d}}_4 &= \gamma_{d4} \left( -\frac{e_1}{\hat{m}_b} \hat{a}_4 - \frac{e_2}{\hat{I}_b} \hat{b}_3 \right) (x_t^r)
\end{aligned}$$

$$\begin{aligned}
\dot{\hat{\theta}}_1 &= \gamma_{\theta 1} \left( -\frac{e_1}{\hat{m}_b} \hat{a}_3 - \frac{e_2}{\hat{I}_b} \hat{b}_3 \right) (\xi_{11}) \\
\dot{\hat{\theta}}_2 &= \gamma_{\theta 2} \left( -\frac{e_1}{\hat{m}_b} \hat{a}_4 - \frac{e_2}{\hat{I}_b} \hat{b}_4 \right) (\xi_{22}) \\
\dot{\hat{\beta}}_1 &= \gamma_{\beta 1} \left( -\frac{e_1}{\hat{m}_b} \hat{a}_3 - \frac{e_2}{\hat{I}_b} \hat{b}_3 \right) (\eta_1) \\
\dot{\hat{\beta}}_2 &= \gamma_{\beta 2} \left( -\frac{e_1}{\hat{m}_b} \hat{a}_3 - \frac{e_2}{\hat{I}_b} \hat{b}_3 \right) (\eta_2) \\
\dot{\hat{\beta}}_3 &= \gamma_{\beta 3} \left( -\frac{e_1}{\hat{m}_b} \hat{a}_4 - \frac{e_2}{\hat{I}_b} \hat{b}_4 \right) (\eta_3) \\
\dot{\hat{\beta}}_4 &= \gamma_{\beta 4} \left( -\frac{e_1}{\hat{m}_b} \hat{a}_4 - \frac{e_2}{\hat{I}_b} \hat{b}_4 \right) (\eta_4) \\
\dot{\hat{A}} &= \gamma_A \left( e_1(V_1 + V_2) + e_2(-aV_1 + bV_2) \right) \\
\dot{\hat{B}} &= \gamma_B \left( -e_1(I_1 + I_2) + e_2(-aI_1 + bI_2) \right) \\
\dot{\hat{C}} &= \gamma_C \left( -e_1(\dot{x}_{su}^f + \dot{x}_{su}^r) + e_2(-ax_{su}^f + bx_{su}^r) \right) \\
\dot{\hat{m}}_b &= \gamma_m \left( \dot{x}_b - \frac{e_1}{\hat{m}_b} (\kappa_1 - \hat{a}_3 - \hat{a}_4) - \frac{e_2}{\hat{I}_b} (-\hat{b}_3 - \hat{b}_4) \right) \left( e_1 + \frac{\psi_1}{\hat{m}_b} \right) \\
\dot{\hat{I}}_n &= \gamma_I \left( \dot{\varrho} - \frac{e_1}{\hat{m}_b} (-a\hat{a}_3 + b\hat{a}_4) - \frac{e_2}{\hat{I}_b} (\kappa_2 - a\hat{a}_3 + b\hat{b}_4) \right) \left( e_2 + \frac{\psi_2}{\hat{I}_b} \right)
\end{aligned} \tag{5.26}$$

The following projections are added to avoid singularity.

$$\begin{aligned}
\dot{\hat{m}}_b &= \begin{cases} 0, & \text{If } \hat{m}_b = 0 \text{ and } \dot{\hat{m}}_b < 0 \\ \dot{\hat{m}}_b, & \text{If } \hat{m}_b = 0 \text{ and } \dot{\hat{m}}_b \geq 0 \\ \dot{\hat{m}}_b & \text{Otherwise} \end{cases} \\
\dot{\hat{I}}_b &= \begin{cases} 0, & \text{If } \hat{I}_b = 0 \text{ and } \dot{\hat{I}}_b < 0 \\ \dot{\hat{I}}_b, & \text{If } \hat{I}_b = 0 \text{ and } \dot{\hat{I}}_b \geq 0 \\ \dot{\hat{I}}_b & \text{Otherwise} \end{cases} \\
\dot{\hat{A}} &= \begin{cases} 0, & \text{If } \hat{A} = 0 \text{ and } \dot{\hat{A}} < 0 \\ \dot{\hat{A}}, & \text{If } \hat{A} = 0 \text{ and } \dot{\hat{A}} \geq 0 \\ \dot{\hat{A}} & \text{Otherwise} \end{cases}
\end{aligned} \tag{5.27}$$

#### 5.4. Stability

**Theorem 5.2.** *Consider the plant (5.13) with the actuator dynamics (5.1),(5.2), the adaptive controllers (5.23) and the update laws (5.26), (5.27). In view of assumptions,*

- (i) *The equilibrium  $\tilde{a}_1, \tilde{a}_2, \tilde{a}_3, \tilde{a}_4, \tilde{a}_{1n}, \tilde{a}_{2n}, \tilde{b}_1, \tilde{b}_2, \tilde{b}_3, \tilde{b}_4, \tilde{b}_{1n}, \tilde{b}_{2n}, \tilde{c}_2, \tilde{c}_4, \tilde{d}_2, \tilde{d}_4, \tilde{m}_b, \tilde{I}_b, \tilde{\theta}_1^T, \tilde{\theta}_2^T, \tilde{\beta}_1^T, \tilde{\beta}_2^T, \tilde{\beta}_3^T, \tilde{\beta}_4^T, \tilde{A}, \tilde{B}$  and  $\tilde{C}$  are stable. The signals  $\ddot{x}_b, \ddot{\varrho}, \dot{e}_1, \dot{e}_2, \ddot{x}_b, \ddot{\varrho}, \dot{e}_1$  and  $\dot{e}_2$  converge to zero while time goes to  $\infty$ .*
- (ii) *The signals  $U_1$  and  $U_1$  are bounded for all initial conditions.*

*Proof.* The following closed loop system is obtained by adding the left hand side of (5.14) and (5.15) into (5.19), then, plugging it into (5.13).

$$\begin{aligned}
\ddot{x}_b &= \kappa_1 \dot{x}_b + \tilde{a}_1 x_{su}^f + \tilde{a}_{1n} (x_{su}^f)^3 + \tilde{a}_2 x_{su}^r + \tilde{a}_{2n} (x_{su}^r)^3 + \tilde{a}_3 \dot{x}_{su}^f + \tilde{a}_4 \dot{x}_{su}^r \\
&\quad + (\hat{m}_b + \tilde{m}_b) e_1 + \frac{\tilde{m}_b}{\hat{m}_b} \psi_1 \\
\ddot{\rho} &= \kappa_2 \dot{\rho} + \tilde{b}_1 x_{su}^f + \tilde{b}_{1n} (x_{su}^f)^3 + \tilde{b}_2 x_{su}^r + \tilde{b}_{2n} (x_{su}^r)^3 + \tilde{b}_3 \dot{x}_{su}^f + \tilde{b}_4 \dot{x}_{su}^r \\
&\quad + (\hat{I}_b + \tilde{I}_b) e_2 + \frac{\tilde{I}_b}{\hat{I}_b} \psi_2
\end{aligned} \tag{5.28}$$

Substituting (5.23) into (5.20) using (5.18);

$$\begin{aligned}
\dot{e}_1 &= -c_1 e_1 + \tilde{A}(V_1 + V_2) - \tilde{B}(I_1 + I_2) - \tilde{C}(\dot{x}_{su}^r + \dot{x}_{su}^f) - \frac{1}{\hat{m}_b} \left( (\kappa_1 - \hat{a}_3 - \hat{a}_4) (\tilde{a}_1 x_{su}^f \right. \\
&\quad + \tilde{a}_{1n} (x_{su}^f)^3 + \tilde{a}_2 x_{su}^r + \tilde{a}_{2n} (x_{su}^r)^3 + \tilde{a}_3 \dot{x}_{su}^f + \tilde{a}_4 \dot{x}_{su}^r + \tilde{m}_b (e_1 + \frac{\psi_1}{\hat{m}_b})) \\
&\quad + \left( -a\hat{a}_3 + b\hat{a}_4 \right) (\tilde{b}_1 x_{su}^f + \tilde{b}_{1n} (x_{su}^f)^3 + \tilde{b}_2 x_{su}^r + \tilde{b}_{2n} (x_{su}^r)^3 + \tilde{b}_3 \dot{x}_{su}^f + \tilde{b}_4 \dot{x}_{su}^r \\
&\quad + \tilde{I}_b (e_2 + \frac{\psi_2}{\hat{I}_b})) + \hat{a}_3 (\tilde{c}_2 x_t^f + \tilde{c}_4 \dot{x}_t^f + \theta_1^T \delta_1 + \tilde{\theta}_1^T \xi_{11} + \tilde{\beta}_1^T \eta_1 + \tilde{\beta}_2^T \eta_2) + \hat{a}_4 (\tilde{d}_2 x_t^r \\
&\quad \left. + \tilde{d}_4 \dot{x}_t^r + \theta_2^T \delta_2 + \tilde{\theta}_2^T \xi_{22} + \tilde{\beta}_3^T \eta_3 + \tilde{\beta}_4^T \eta_4) \right) \\
\dot{e}_2 &= -c_2 e_2 + \tilde{A}(-aV_1 + bV_2) - \tilde{B}(-aI_1 + bI_2) - \tilde{C}(-a\dot{x}_{su}^r + b\dot{x}_{su}^f) - \frac{1}{\hat{I}_b} \left( (\kappa_2 - \hat{a}b_3 \right. \\
&\quad + \hat{b}b_4) (\tilde{b}_1 x_{su}^f + \tilde{b}_{1n} (x_{su}^f)^3 + \tilde{b}_2 x_{su}^r + \tilde{b}_{2n} (x_{su}^r)^3 + \tilde{b}_3 \dot{x}_{su}^f + \tilde{b}_4 \dot{x}_{su}^r + \tilde{I}_b (e_2 + \frac{\psi_2}{\hat{I}_b})) \\
&\quad + \left( -\hat{b}_3 - \hat{b}_4 \right) (\tilde{a}_1 x_{su}^f + \tilde{a}_{1n} (x_{su}^f)^3 + \tilde{a}_2 x_{su}^r + \tilde{a}_{2n} (x_{su}^r)^3 + \tilde{a}_3 \dot{x}_{su}^f + \tilde{a}_4 \dot{x}_{su}^r \\
&\quad + \tilde{m}_b (e_1 + \frac{\psi_1}{\hat{m}_b})) + \hat{b}_3 (\tilde{c}_2 x_t^f + \tilde{c}_4 \dot{x}_t^f + \theta_1^T \delta_1 + \tilde{\theta}_1^T \xi_{11} + \tilde{\beta}_1^T \eta_1 + \tilde{\beta}_2^T \eta_2) + \hat{b}_4 (\tilde{d}_2 x_t^r \\
&\quad \left. + \tilde{d}_4 \dot{x}_t^r + \theta_2^T \delta_2 + \tilde{\theta}_2^T \xi_{22} + \tilde{\beta}_3^T \eta_3 + \tilde{\beta}_4^T \eta_4) \right)
\end{aligned} \tag{5.29}$$

Using the following Lyapunov function, the stability of the closed loop plant is established;

$$\begin{aligned}
V = \frac{1}{2} & \left( \dot{x}_b^2 + \dot{\varrho}^2 + e_1^2 + e_2^2 + \tilde{a}_1^2 + \tilde{a}_2^2 + \tilde{a}_3^2 + \tilde{a}_4^2 + \tilde{a}_{1n}^2 + \tilde{a}_{2n}^2 + \tilde{b}_1^2 + \tilde{b}_2^2 + \tilde{b}_3^2 + \tilde{b}_4^2 + \tilde{b}_{1n}^2 \right. \\
& + \tilde{b}_{2n}^2 + \tilde{c}_2^2 + \tilde{c}_4^2 + \tilde{d}_2^2 + \tilde{d}_4^2 + \tilde{A}^2 + \tilde{B}^2 + \tilde{C}^2 + \tilde{m}_b^2 + \tilde{I}_b^2 + \tilde{\theta}_1^T \tilde{\theta}_1 + \tilde{\theta}_2^T \tilde{\theta}_2 + \tilde{\beta}_1^T \tilde{\beta}_1 \\
& \left. + \tilde{\beta}_2^T \tilde{\beta}_2 + \tilde{\beta}_3^T \tilde{\beta}_3 + \tilde{\beta}_4^T \tilde{\beta}_4 + \delta_1^T P_{G_1} \delta_1 + \delta_2^T P_{G_2} \delta_2 \right) \quad (5.30)
\end{aligned}$$

where;

$$G_1^T P_{G_1} + P_{G_1} G_1 = -2\epsilon_1 I \quad (5.31)$$

$$G_2^T P_{G_2} + P_{G_2} G_2 = -2\epsilon_2 I \quad (5.32)$$

Taking the derivative of V, with using (5.28), (5.29), (5.26), (5.27) and (5.8);

$$\begin{aligned}
\dot{V} = & \kappa_1 \dot{x}_b^2 + \kappa_2 \dot{\varrho}^2 - c_1 e_1^2 - c_2 e_2^2 - \frac{e_1}{\hat{m}_b} \left( \hat{a}_3 \theta_1^T \delta_1 + \hat{a}_4 \theta_2^T \delta_2 \right) - \frac{e_2}{\hat{I}_b} \left( \hat{b}_3 \theta_1^T \delta_1 + \hat{b}_4 \theta_2^T \delta_2 \right) \\
& - c_2 e_2^2 + \epsilon_1 \delta_1^T \delta_1 + \epsilon_2 \delta_2^T \delta_2 \quad (5.33)
\end{aligned}$$

To handle the cross terms, Young's inequality is applied;

$$\frac{e_1}{\hat{m}_b} \hat{a}_3 \theta_1^T \delta_1 \leq \frac{e_1^2 \hat{a}_3^2}{2 \hat{m}_b^2} + \frac{\lambda_{\max}(\theta_1 \theta_1^T) \delta_1^T \delta_1}{2} \quad (5.34)$$

$$\frac{e_1}{\hat{m}_b} \hat{a}_4 \theta_2^T \delta_2 \leq \frac{e_1^2 \hat{a}_4^2}{2 \hat{m}_b^2} + \frac{\lambda_{\max}(\theta_2 \theta_2^T) \delta_2^T \delta_2}{2} \quad (5.35)$$

$$\frac{e_2}{\hat{I}_b} \hat{b}_3 \theta_1^T \delta_1 \leq \frac{e_2^2 \hat{b}_3^2}{2 \hat{I}_b^2} + \frac{\lambda_{\max}(\theta_1 \theta_1^T) \delta_1^T \delta_1}{2} \quad (5.36)$$

$$\frac{e_2}{\hat{I}_b} \hat{b}_4 \theta_2^T \delta_2 \leq \frac{e_2^2 \hat{b}_4^2}{2 \hat{I}_b^2} + \frac{\lambda_{\max}(\theta_2 \theta_2^T) \delta_2^T \delta_2}{2} \quad (5.37)$$

By choosing,  $c_1 = 1 + \frac{\hat{a}_3^2}{2\hat{m}_b^2} + \frac{\hat{a}_4^2}{2\hat{m}_b^2}$ ,  $c_2 = 1 + \frac{\hat{b}_3^2}{2\hat{m}_b^2} + \frac{\hat{b}_4^2}{2\hat{m}_b^2}$ ,  $\epsilon_1 = -1 - \lambda_{max}(\theta_1\theta_1^T)$  and  $\epsilon_2 = -1 - \lambda_{max}(\theta_2\theta_2^T)$ , we obtain,

$$\dot{V} \leq \kappa_1 \dot{x}_b^2 + \kappa_2 \dot{\varrho}^2 - c_1 e_1^2 - c_2 e_2^2 - \epsilon_1 \delta_1 - \epsilon_2 \delta_2 \quad (5.38)$$

then, it is concluded;

$$V(t) \leq V(0) \quad (5.39)$$

which tells us that V is bounded.

Defining;

$$\varpi = \begin{bmatrix} \dot{z} & \ddot{z} & \dot{\varrho} & \ddot{\varrho} & e_1 & e_2 & \tilde{a}_1 & \tilde{a}_2 & \tilde{a}_3 & \tilde{a}_4 & \tilde{a}_{1n} & \tilde{a}_{2n} & \tilde{b}_1 & \tilde{b}_2 & \tilde{b}_3 & \tilde{b}_4 & \tilde{b}_{1n} & \tilde{b}_{2n} \\ \tilde{c}_2 & \tilde{c}_4 & \tilde{d}_2 & \tilde{d}_4 & \tilde{m} & \tilde{I}_n & \tilde{\theta}_1^T & \tilde{\theta}_2^T & \tilde{\beta}_1^T & \tilde{\beta}_2^T & \tilde{\beta}_3^T & \tilde{\beta}_4^T & \delta_1 & \delta_2 & \tilde{A} & \tilde{B} & \tilde{C} \end{bmatrix} \quad (5.40)$$

Considering 5.30 and 5.39 the following is obtained;

$$|\varpi|^2 \leq M_1 |\varpi(0)|^2 \quad (5.41)$$

where  $M_1 > 0$ .

$\forall \varpi$ , the right hand side of (5.12), (5.18) and (5.28) are continuous in  $\varpi$  and time, which tells us that the right hand side of (5.39) is continuous in  $\varpi$  and time. Moreover, the right hand side of (5.39) is zero when  $\varpi$  is zero. By using Lasalle-Yoshisawa theorem [13], (5.39) assures that  $\dot{x}_b$ ,  $\dot{\varrho}$ ,  $e_1$ ,  $e_2$ ,  $\delta_1$  and  $\delta_2$  converge to zero while time goes to  $\infty$ . From the boundedness and the convergence of  $\dot{x}_b$ ,  $\dot{\varrho}$ ,  $e_1$  and  $e_2$ , it can be concluded that  $\ddot{x}_b$ ,  $\ddot{\varrho}$ ,  $\dot{e}_1$  and  $\dot{e}_2$  converge to zero while time goes to  $\infty$ . In addition, in the light of the boundedness of the suspension gap for both tires and the boundedness of  $\dot{X}_b$ , it is concluded that  $X_t$  and  $\dot{X}_t$  are bounded.

Because of the fact that the road disturbance consists of a sum of sinusoidal (2.42),  $\nu_1$  and  $\nu_2$  are bounded, noticing that  $G$  is Hurwitz, then, it is concluded that  $\delta_1$  and  $\delta_2$  are bounded (5.12). Additionally, we can say that  $\xi_{11}$ ,  $\xi_{22}$ ,  $\eta_1$ ,  $\eta_2$ ,  $\eta_3$  and  $\eta_4$  are bounded with using (5.6), which leads to the boundedness of  $\theta_1^T$ ,  $\beta_1^T$ ,  $\beta_2^T$ ,  $\theta_2^T$ ,  $\beta_3^T$  and  $\beta_4^T$  are bounded from (5.4) and (5.5). Since  $\tilde{a}_1$ ,  $\tilde{a}_2$ ,  $\tilde{a}_3$ ,  $\tilde{a}_4$ ,  $\tilde{a}_{1n}$ ,  $\tilde{a}_{2n}$ ,  $\tilde{b}_1$ ,  $\tilde{b}_2$ ,  $\tilde{b}_3$ ,  $\tilde{b}_4$ ,  $\tilde{b}_{1n}$ ,  $\tilde{b}_{2n}$ ,  $\tilde{c}_2$ ,  $\tilde{c}_4$ ,  $\tilde{d}_2$ ,  $\tilde{d}_4$ ,  $\tilde{m}_b$ ,  $\tilde{I}_b$ ,  $\tilde{\theta}_1^T$ ,  $\tilde{\theta}_2^T$ ,  $\tilde{\beta}_1^T$ ,  $\tilde{\beta}_2^T$ ,  $\tilde{\beta}_3^T$ ,  $\tilde{\beta}_4^T$ ,  $\tilde{A}$ ,  $\tilde{B}$  and  $\tilde{C}$  are bounded, estimations ( $\hat{a}_1$ ,  $\hat{a}_2$ ,  $\hat{a}_3$ ,  $\hat{a}_4$ ,  $\hat{a}_{1n}$ ,  $\hat{a}_{2n}$ ,  $\hat{b}_1$ ,  $\hat{b}_2$ ,  $\hat{b}_3$ ,  $\hat{b}_4$ ,  $\hat{b}_{1n}$ ,  $\hat{b}_{2n}$ ,  $\hat{c}_2$ ,  $\hat{c}_4$ ,  $\hat{d}_2$ ,  $\hat{d}_4$ ,  $\hat{m}_b$ ,  $\hat{I}_b$ ,  $\hat{\theta}_1^T$ ,  $\hat{\theta}_2^T$ ,  $\hat{\beta}_1^T$ ,  $\hat{\beta}_2^T$ ,  $\hat{\beta}_3^T$ ,  $\hat{\beta}_4^T$ ,  $\hat{A}$ ,  $\hat{B}$  and  $\hat{C}$ ) are bounded considering (5.18). Furthermore, bearing in mind that  $K$  is a negative definite matrix, estimations are bounded, it is concluded that  $U_{1d}$  and  $U_{2d}$  are bounded with using (5.14) and (5.15). Then, it is attained that  $U_1$  and  $U_2$  are bounded.  $\square$

## 5.5. Simulation

To reveal the performance of the controller, a simulation is prepared. The parameters of the plant are taken from Appendix C. Considering the half car model contains the dynamics of front and rear tire, the road disturbance input is given in the following;

$$\nu_1 = \begin{cases} 0 & 0 \leq t \leq 12 \\ \nu_{d1} & 12 < t \leq 24 \\ 0 & 24 < t \leq 34 \\ \nu_{d2} & 34 < t \leq 45 \\ 0 & 45 < t \leq 50 \end{cases} \quad \nu_2 = \begin{cases} 0 & 0 \leq t \leq 12 \\ \nu_{d1} & 12 < t \leq 24 \\ 0 & 24 < t \leq 34 \\ \nu_{d2} & 34 < t \leq 45 \\ 0 & 45 < t \leq 50 \end{cases} \quad (5.42)$$

where;

$$\begin{aligned} \nu_{d1} &= 0.03 \sin(2\pi t) + 0.02 \sin(1.5\pi t + \frac{\pi}{6}) \\ \nu_{d2} &= 0.03 \sin(15\pi t) + 0.02 \sin(10\pi t + \frac{\pi}{6}) \end{aligned} \quad (5.43)$$

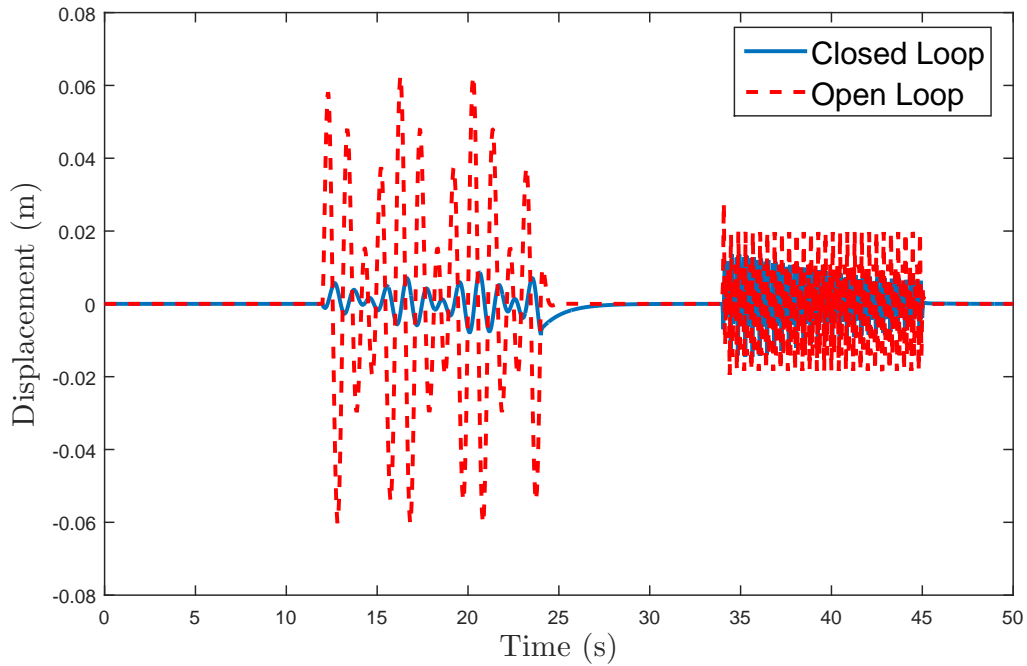


Figure 5.1. The displacement response of the body.

It is assumed that the front and the rear tires are exposed to same road profile with considering the time delay between them. Initial conditions are taken as zeros, except the singular terms. The road test contains high and low frequency waves to represent harsh real life environment.

Figure 5.1 and 5.2 display the displacement and acceleration response of the body. The displacement of the body is decreased with active suspension (Closed Loop), which leads to improve the performance of the vehicle. ISO 2631 states that the vertical acceleration affects the comfort of the passengers [12]. It is clear that the active suspension system offers more smooth ride than the passive system.

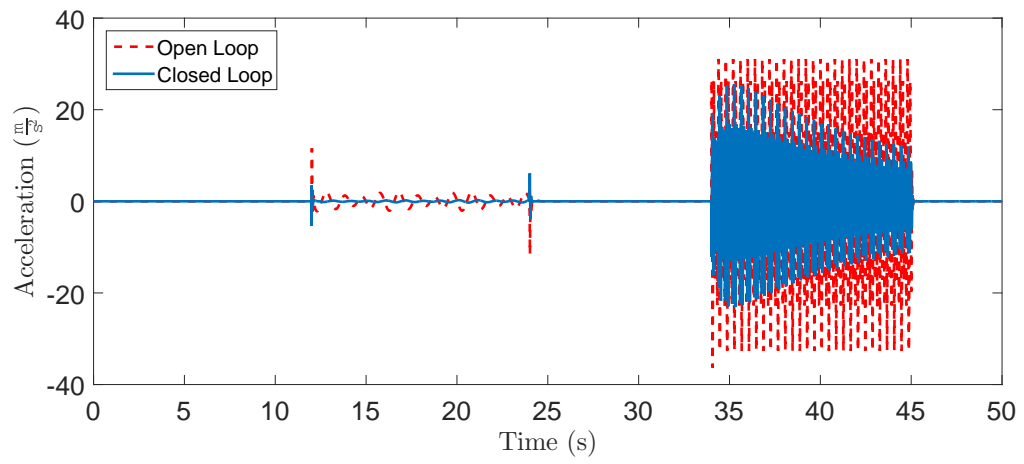


Figure 5.2. The acceleration response of the body.

## 6. CASE STUDY

In this chapter, the simulation results of the quarter and half car model are discussed. Numerical studies are conducted to evaluate the performance of the designed controller for an active suspension system. In order to demonstrate the dynamic characteristic of the vehicle, it is assumed that the vehicle is exposed to sinusoidal or random road inputs. In Section 2.4, we design an observer to compensate the road disturbance where the parameters of the sinusoidal wave are considered as unknown. To demonstrate the effectiveness of the observer, the random road disturbance, which is given in Section 2.5, is applied to the half car model.

The half car model (2.39) is simulated with the road disturbance observers (5.4), (5.5) and the adaptive controllers (5.14), (5.15). The parameters of the system are given in Appendix 1. It is assumed that the rear and front tire are travel same road profile. However, the rear tire experience a delay which is represented by  $\Delta t = \frac{l}{v}$ , where  $l$  is the length of an wheelbase,  $v$  is a speed of the vehicle. For the simulation,  $l = 0.96m$  and  $v = 100km/h$  are chosen. E grade is selected for the road roughness. The length of the road is 200m. The values of the road roughness is given in Table 6.1, where A represents the excellent road quality. On the other hand, E represents very poor road quality. ISO 2631 states that the duration of a comfort evaluation analysis is 5 seconds. The road input is given in Figure 2.5.

Figure 6.1 and 6.5 illustrate the acceleration and the displacement of the body, respectively, where the open loop (passive suspension) and the closed loop (active suspension) are compared. It is clear that the closed loop system demonstrates better performance than open loop system in terms of the isolation of the body from the road disturbance despite the limited information such as uncertain parameters and unmeasured states.

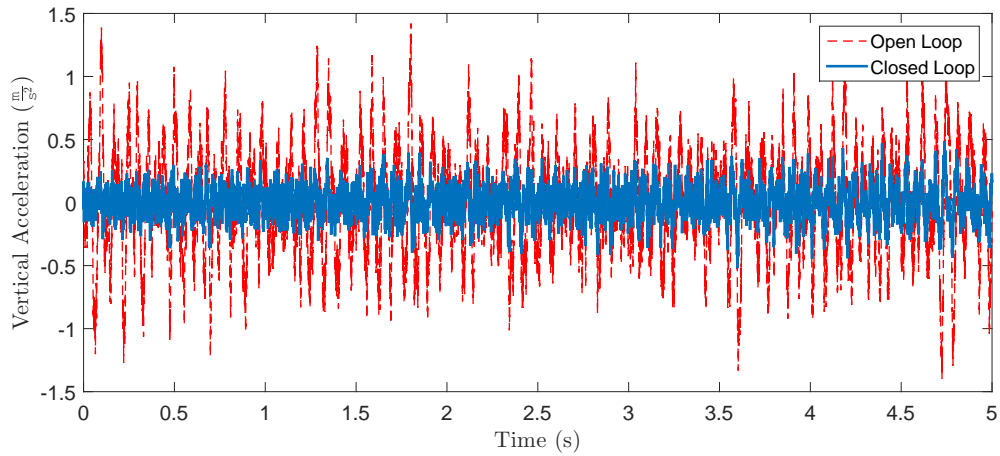


Figure 6.1. The acceleration response of the body to random road input.

Table 6.1. Road Roughness Values According to ISO 8608.

road class	lower limit ( $10^{-6}$ )	geometric mean ( $10^{-6}$ )	upper limit ( $10^{-6}$ )
A	-	16	32
B	32	64	128
C	128	256	512
D	512	1024	2048
E	2048	4096	8192

### 6.1. The Evaluation of RMS Value

The comfort of the passengers is heavily depends on the RMS value of the acceleration of the body [19] . To evaluate the performance of the controller, RMS (Root Mean Square) values are investigated for body pitch and heave responses. The RMS value can be obtained in the following [12];

$$a_w = \left[ \frac{1}{T} \int_0^T a_w^2(t) dt \right]^{1/2} \quad (6.1)$$

In (6.1), T represents the exposed time of the disturbance,  $a_w$  denotes the weighted acceleration.

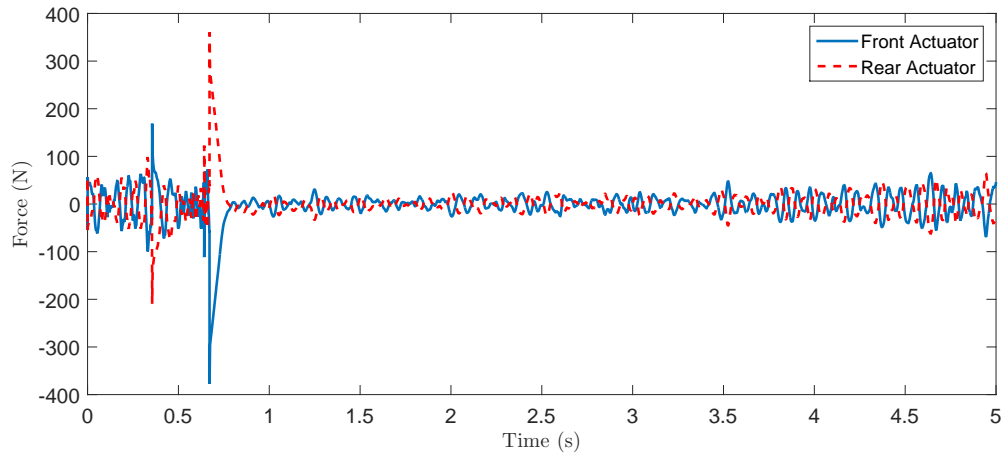


Figure 6.2. Actuator responses.

Table 6.2. Comfort Reactions According to ISO 2631.

The RMS value of Vertical Acceleration ( $m/s^2$ )	Perceived Comfort
$a_w < 0.315$	not uncomfortable
$0.315 < a_w < 0.63$	a little uncomfortable
$0.63 < a_w < 1$	fairly uncomfortable
$1 < a_w < 1.6$	uncomfortable
$1.6 < a_w < 2.5$	very uncomfortable
$a_w > 2.5$	extremely uncomfortable

Figure 6.8 illustrates the RMS values of heave motion of the vehicle for open and closed loop responses. It is clear that there is a significant decrease of the perceived acceleration by passengers with using the proposed controller. The vertical acceleration response is improved 69% by using closed loop system. Table 6.2 shows the comfort perception of passengers in terms of acceleration. The RMS value of open loop response (0.3884) is perceived a little uncomfortable by passengers. With the help of the active suspension, the closed loop response (0.1201) demonstrates a comfortable ride.

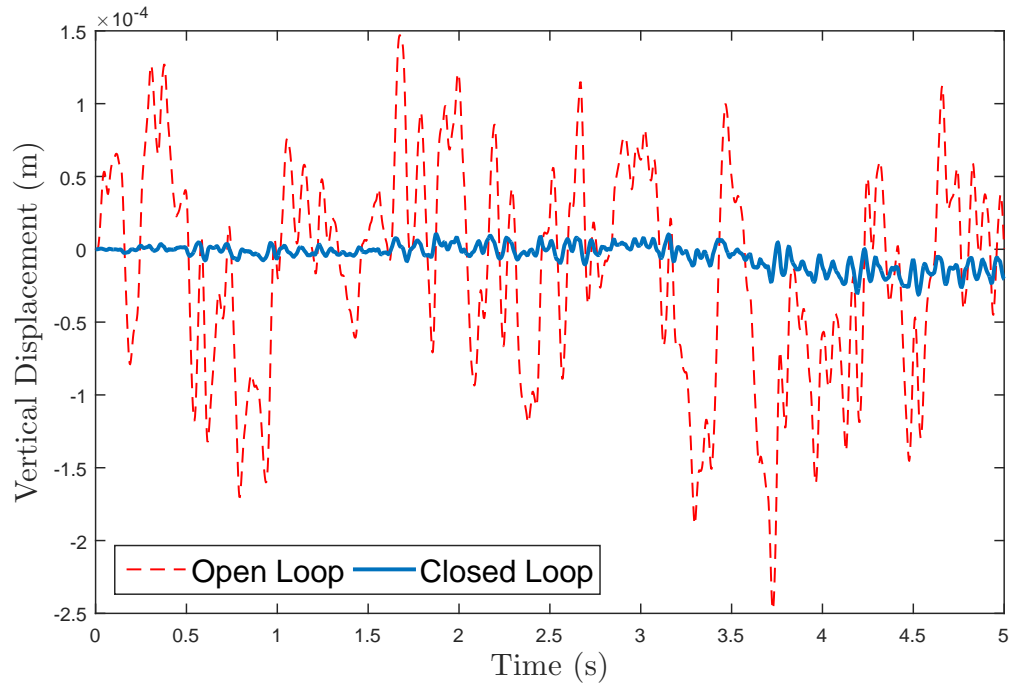


Figure 6.3. The displacement response of the body to random road input.

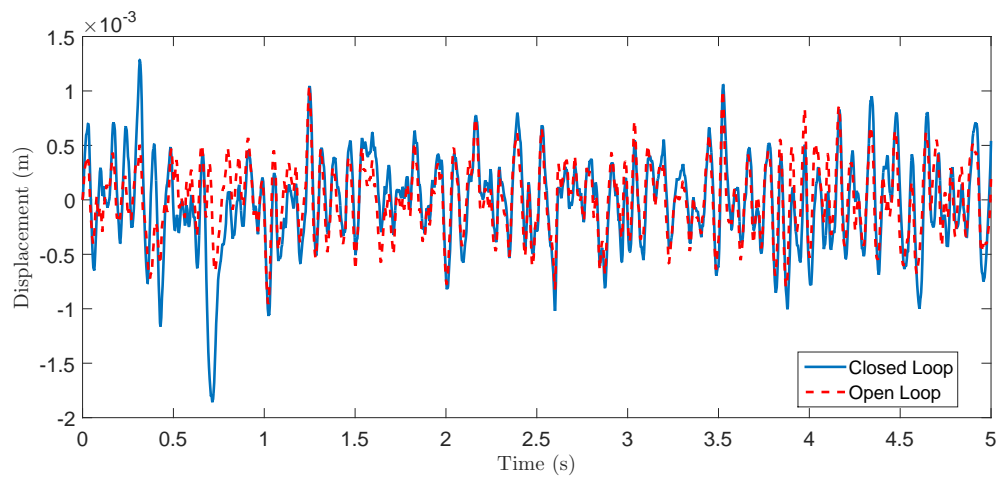


Figure 6.4. Relative displacement between the body and the front tire.

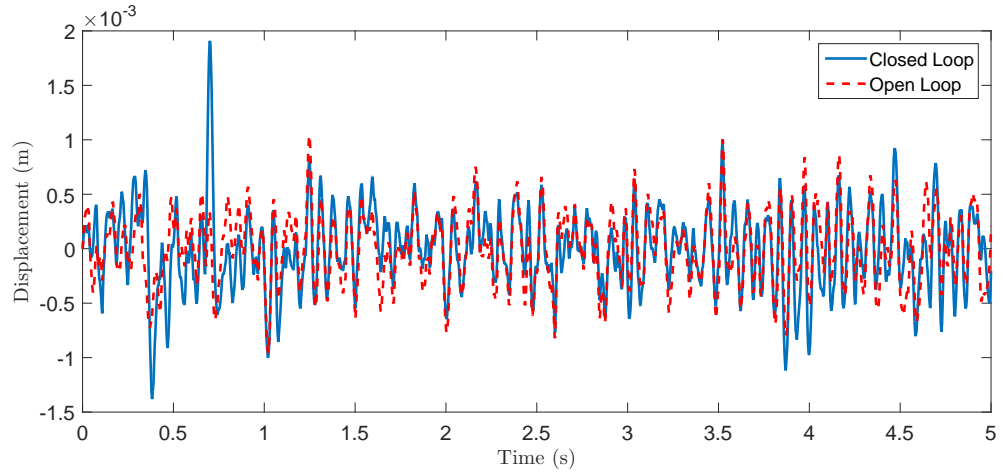


Figure 6.5. Relative displacement between the body and the rear tire.

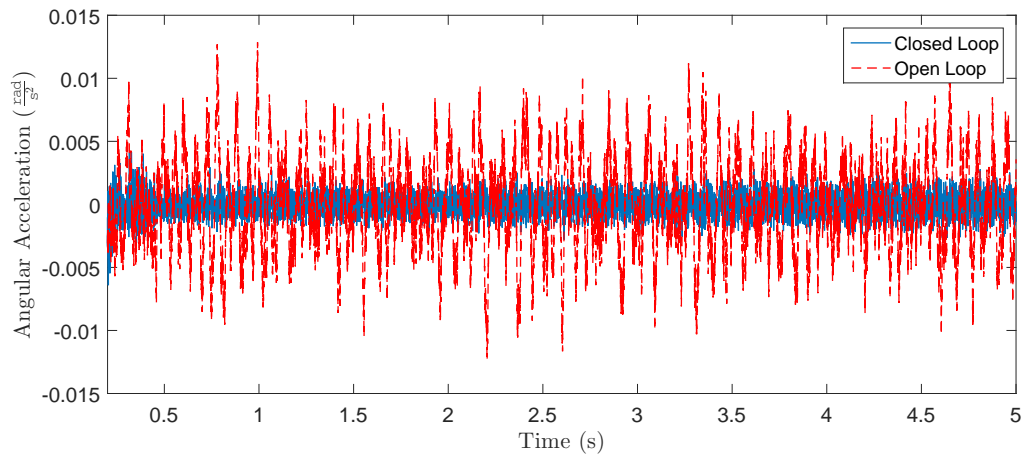


Figure 6.6. The angular acceleration of the pitch motion.

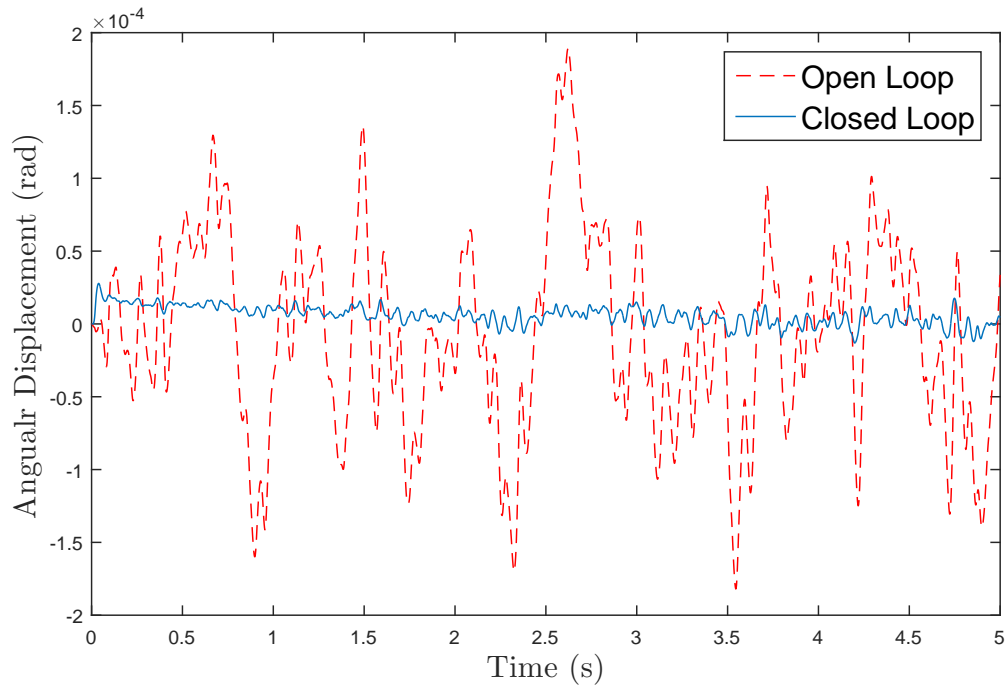


Figure 6.7. The angular displacement of the pitch motion to random road input.

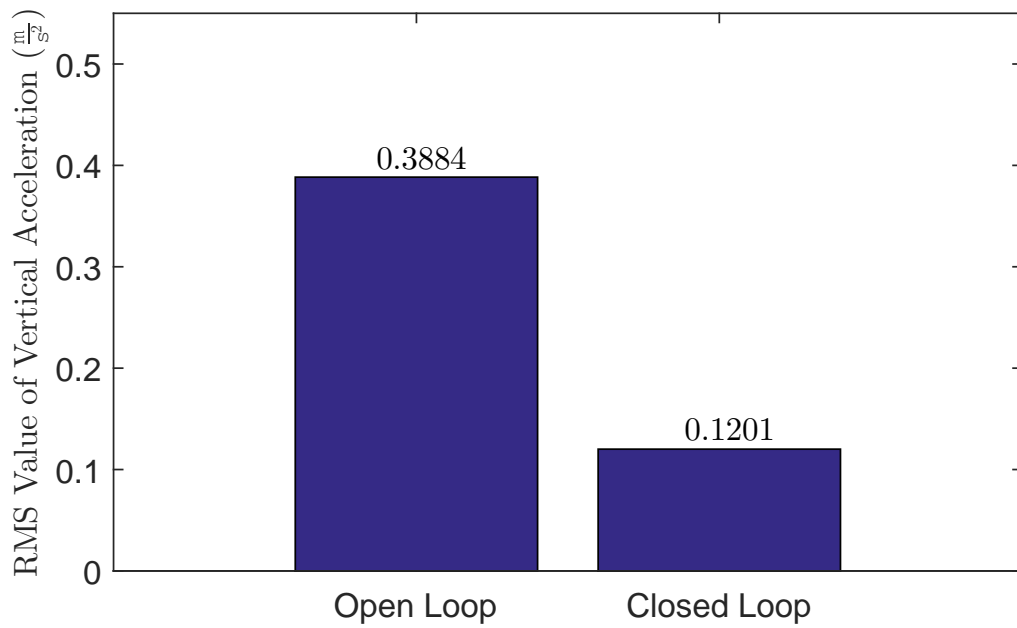


Figure 6.8. The RMS values of heave acceleration for random road input.

## 7. CONCLUSIONS

In this thesis, three different types of controller are discussed with using adaptive backstepping control to isolate the vehicle body from road disturbance. The mathematical models are developed for a seat, a quarter and a half vehicle model.

Firstly, a controller is designed for a basic seat model where the road disturbance is considered as unknown. The observer is designed to compensate the unknown road disturbance. Moreover, a quarter car model, which considers the dynamic behaviour of the tire, is investigated. In addition to the unknown disturbance, the parameters of the tire, which can be easily changed by wear and tear, and the mass of the body, which also can be changed by the payload or the number of the passengers, are considered as unknown in the quarter car model. Another improvement is that the dynamics of the electromagnetic actuator is considered. Lastly, a controller for a half car model is presented. In the half car model, the nonlinear behaviour of the spring is taken into consideration. Furthermore, partial states, which are the vertical and angular velocities of the body, suspension gaps and the displacements and velocities of the tires are assumed to be measured. Therefore, with reducing of the number of sensors, the implementation cost of the system is decreased. The mass of the body and the parameters of the tire are considered as unknown and the dynamics of the actuator is considered same as the quarter car model.

In simulation part, the road test is applied to the half car model. The random road profile is generated with using ISO 8608 standard. The designed adaptive backstepping controller performs much better than the uncontrolled case. The RMS values are  $0.3884 \left(\frac{m}{s^2}\right)$  for open loop and  $0.1201 \left(\frac{m}{s^2}\right)$  for closed loop system. The vertical acceleration response is improved 69% by using the proposed adaptive controller.

For future, the study can be extended to consider time delay. In this way, the real life application is more realizable. This thesis does not mention the frequency domain response. Therefore, it can be added. Furthermore, the designed controller can be implemented on a test rig to observe the performance of the proposed controller.

## REFERENCES

1. Koch, G. P., *Adaptive control of mechatronic vehicle suspension systems*, Ph.D. Thesis, Universität München, 2011.
2. Montazeri-Gh, M. and M. Soleymani, “Investigation of the energy regeneration of active suspension system in hybrid electric vehicles”, *IEEE transactions on industrial electronics*, Vol. 57, No. 3, pp. 918–925, 2010.
3. Kumar, M. S., “Development of active suspension system for automobiles using PID controller”, *Citeseer*, 2008.
4. “Road safety: Despite progress deaths remain too high. (n.d.)”, <http://www.who.int/mediacentre/news/releases/2015/road-safety-report/en/>, accessed at April 2017.
5. Aly, A. A. and F. A. Salem, “Vehicle suspension systems control: A review”, *International journal of control, automation and systems*, Vol. 2, No. 2, pp. 46–54, 2013.
6. Fischer, D. and R. Isermann, “Mechatronic semi-active and active vehicle suspensions”, *Control engineering practice*, Vol. 12, No. 11, pp. 1353–1367, 2004.
7. Simon, D. E., *Experimental evaluation of semiactive magnetorheological primary suspensions for heavy truck applications*, Ph.D. Thesis, Virginia Tech, 1998.
8. Mailat, F., Ş. Donescu and V. Chiroiu, “On the automotive semi-active suspensions”, *Proc. of the Romanian Academy, Series A: Mathematics, Physics, Technical Sciences, Information Science*, Vol. 5, No. 1, pp. 47–54, 2004.

9. Lefebvre, D., P. Chevrel and S. Richard, “An H-infinity-based control design methodology dedicated to the active control of vehicle longitudinal oscillations”, *IEEE transactions on control systems technology*, Vol. 11, No. 6, pp. 948–956, 2003.
10. Li, H., H. Liu, H. Gao and P. Shi, “Reliable fuzzy control for active suspension systems with actuator delay and fault”, *IEEE Transactions on Fuzzy Systems*, Vol. 20, No. 2, pp. 342–357, 2012.
11. Li, H., J. Yu, C. Hilton and H. Liu, “Adaptive sliding-mode control for nonlinear active suspension vehicle systems using T–S fuzzy approach”, *IEEE Transactions on Industrial Electronics*, Vol. 60, No. 8, pp. 3328–3338, 2013.
12. ISO, *Mechanical Vibration and Shock: Evaluation of Human Exposure to Whole-body Vibration. Part 1, General Requirements: International Standard ISO 2631-1: 1997 (E)*, ISO, 1997.
13. Krstic, M., I. Kanellakopoulos and P. V. Kokotovic, *Nonlinear and adaptive control design*, Wiley, 1995.
14. Fierro, R. and F. L. Lewis, “Control of a nonholonomic mobile robot: backstepping kinematics into dynamics”, *Decision and Control, 1995., Proceedings of the 34th IEEE Conference on*, Vol. 4, pp. 3805–3810, IEEE, 1995.
15. Madani, T. and A. Benallegue, “Backstepping control for a quadrotor helicopter”, *Intelligent Robots and Systems, 2006 IEEE/RSJ International Conference on*, pp. 3255–3260, IEEE, 2006.
16. Farrell, J., M. Sharma and M. Polycarpou, “Backstepping-based flight control with adaptive function approximation”, *Journal of Guidance, Control, and Dynamics*, Vol. 28, No. 6, pp. 1089–1102, 2005.

17. Lin, J.-S. and I. Kanellakopoulos, “Nonlinear design of active suspensions”, *Decision and Control, 1995., Proceedings of the 34th IEEE Conference on*, Vol. 4, pp. 3567–3569, IEEE, 1995.
18. Huang, C.-J. and J.-S. Lin, “Nonlinear active suspension control design applied to a half-car model”, *Networking, Sensing and Control, 2004 IEEE International Conference on*, Vol. 2, pp. 719–724, IEEE, 2004.
19. Yagiz, N. and Y. Hacioglu, “Backstepping control of a vehicle with active suspensions”, *Control Engineering Practice*, Vol. 16, No. 12, pp. 1457–1467, 2008.
20. Karlsson, N., A. Teel and D. Hrovat, “A backstepping approach to control of active suspensions”, *Decision and Control, 2001. Proceedings of the 40th IEEE Conference on*, Vol. 5, pp. 4170–4175, IEEE, 2001.
21. Sun, W., H. Gao and O. Kaynak, “Adaptive backstepping control for active suspension systems with hard constraints”, *IEEE/ASME transactions on mechatronics*, Vol. 18, No. 3, pp. 1072–1079, 2013.
22. Sun, W., H. Pan, Y. Zhang and H. Gao, “Multi-objective control for uncertain nonlinear active suspension systems”, *Mechatronics*, Vol. 24, No. 4, pp. 318–327, 2014.
23. Basturk, H. I., “A backstepping approach for an active suspension system”, *American Control Conference (ACC), 2016*, pp. 7579–7584, IEEE, 2016.
24. Baştürk, H. İ. and M. Krstic, “Adaptive cancelation of matched unknown sinusoidal disturbances for unknown LTI systems by state derivative feedback”, *American Control Conference (ACC), 2012*, pp. 1149–1154, IEEE, 2012.
25. Nikiforov, V. O., “Observers of external deterministic disturbances. I. objects with known parameters”, *Automation and Remote Control*, Vol. 65, No. 10, pp. 1531–1541, 2004.

26. Baruh, H., “Analytical dynamics, WCB”, *McGraw-Hill*, Vol. 6, p. 21, 1999.
27. Meirovitch, L., “Fundamentals of vibrations. 2001”, *International Edition*, *McGraw-Hill*, 2000.
28. Gysen, B. L., J. J. Paulides, J. L. Janssen and E. A. Lomonova, “Active electromagnetic suspension system for improved vehicle dynamics”, *IEEE Transactions on Vehicular Technology*, Vol. 59, No. 3, pp. 1156–1163, 2010.
29. Michail, K., A. C. Zolotas and R. M. Goodall, “Optimised sensor selection for control and fault tolerance of electromagnetic suspension systems: A robust loop shaping approach”, *ISA transactions*, Vol. 53, No. 1, pp. 97–109, 2014.
30. Van Der Sande, T., “Control of an automotive electromagnetic suspension system”, *Master’s thesis*, *Eindhoven University of Technology*, 2011.
31. Nikiforov, V. O., “Observers of external deterministic disturbances. II. objects with unknown parameters”, *Automation and Remote Control*, Vol. 65, No. 11, pp. 1724–1732, 2004.
32. Tyan, F., Y.-F. Hong, S.-H. Tu and W. S. Jeng, “Generation of random road profiles”, *Journal of Advanced Engineering*, Vol. 4, No. 2, pp. 1373–1378, 2009.
33. Du, H., W. Li and N. Zhang, “Integrated seat and suspension control for a quarter car with driver model”, *IEEE transactions on vehicular technology*, Vol. 61, No. 9, pp. 3893–3908, 2012.

## APPENDIX A: PARAMETERS OF THE SEAT MODEL

Table A.1. Parameter values for the seat model.

	Value	Symbol
mass of the seat	100 <i>kg</i>	m
stiffness coefficient	6800 $\frac{N}{m}$	k
damping coefficient	100 $\frac{N}{ms}$	c
controller gain	$\begin{bmatrix} -7.5 \\ -5.5 \end{bmatrix}$	K
Observer Parameters	$\begin{bmatrix} -1 & 0 & 0 & 0 \\ 0 & -2 & 0 & 0 \\ 0 & 0 & -3 & 0 \\ 0 & 0 & 0 & -4 \end{bmatrix}$	G
	$\begin{bmatrix} 1 & 2 & 3 & 4 \end{bmatrix}^T$	l

## APPENDIX B: PARAMETERS OF THE QUARTER CAR MODEL

Table B.1. Parameter values for the quarter car model [28].

	Value	Symbol
mass of the body	91.23 <i>kg</i>	$m_s$
mass of the tire	22.15 <i>kg</i>	$m_u$
spring coefficient for suspension	6952 $\frac{N}{m}$	$k_s$
spring coefficient for tire	178000 $\frac{N}{m}$	$k_u$
damping coefficient for suspension	1152 $\frac{N}{ms}$	$c_s$
damping coefficient for tire	123 $\frac{N}{ms}$	$c_u$
controller gain	$\begin{bmatrix} -2 \\ -3 \end{bmatrix}$	K
positive definite matrix	$\begin{bmatrix} 3.75 & 0.75 \\ 0.75 & 0.75 \end{bmatrix}$	P
observer parameters	$\begin{bmatrix} -1 & 0 & 0 & 0 \\ 0 & -2 & 0 & 0 \\ 0 & 0 & -3 & 0 \\ 0 & 0 & 0 & -4 \end{bmatrix}$	G
	$\begin{bmatrix} 1 & 2 & 3 & 4 \end{bmatrix}^T$	l

## APPENDIX C: PARAMETERS OF THE HALF CAR

Table C.1. Parameter values for the half car model.

	Value	Symbol
controller gain for $\ddot{x}_b$	-18.59	$\kappa_1$
controller gain for $\ddot{\varrho}$	-12.509	$\kappa_2$
$e_1$ coefficient	800	$c_{e1}$
$e_2$ coefficient	800	$c_{e2}$
mass of the body	182.46 kg	$m_s$
masses of the front and the rear tire	22.5 kg	$m_f, m_r$
spring coefficients for the front and the rear suspension	$6952 \frac{N}{m}$	$k_1, k_2$
nonlinear spring coefficients for the front and the rear suspension	$500 \frac{N}{m}$	$k_{n1}, k_{n2}$
Inertia of the body	$375.176 \text{ kg}\cdot\text{m}^2$	$I_n$
damping coefficients for the front and the rear suspension	$1152 \frac{N}{ms}$	$c_1, c_2$
damping coefficients for the front and the rear tire	$123 \frac{N}{ms}$	$c_t$
spring coefficients for the front and the rear tire	$178000 \frac{N}{m}$	$k_t$
distance between the front tire and the center of gravity	0.48 m	a
distance between the rear tire and the center of gravity	0.44 m	b

## APPENDIX D: PARAMETERS OF THE ACTUATOR MODEL

Table D.1. Parameter values for the actuator [28].

	Value	Symbol
resistance	17 ohm	R
inductance	10 H	$l_c$
force coefficient	115	$k_i$
velocity coefficient	76.6	$k_e$